Dioxygen Activation by Enzymes with Mononuclear Non-Heme Iron Active Sites

Lawrence Que, Jr.,* and Raymond Y. N. Ho

Department of Chemistry, University of Minnesota, Minneapolis, Minnesota 55455

Received April 9, 1996 (Revised Manuscript Received August 5, 1996)

Contents

Lawrence Que, Jr., did his undergraduate work at Ateneo de Manila University (B.S. in 1969) and pursued graduate studies at the University of Minnesota under Professor Louis H. Pignolet (Ph.D. in 1973). After postdoctoral stints with Professors Richard H. Holm at M.I.T. and Eckard Münck at the University of Minnesota, he joined the Cornell University faculty as an Assistant Professor of Chemistry. In 1983 he returned to the University of Minnesota, where he is now Professor of Chemistry and Codirector of the Center for Metals in Biocatalysis. His research has focused on the interface between inorganic chemistry and biology with particular emphasis on understanding the mechanisms of dioxygen activation by non-heme iron enzymes and synthesizing structural, spectroscopic, and functional models of these enzymes.

Raymond Yuen Nang Ho, born in Hong Kong in 1967, received his B.S. degree from the College of Chemistry at University of California, Berkeley, in 1988, where he did research under Dr. Richard Fish. From there, he moved down the coast to the University of California, Los Angeles, where he did his graduate studies under Professor Joan S. Valentine (Ph.D. in 1995). For postdoctoral research, he left the haven of California and journeyed to the University of Minnesota, where he is currently working under Prof. Lawrence Que, Jr. His research interest are in bioinorganic chemistry, where he strives to elucidate the mechanisms of non-heme iron enzymes by studying both the enzymes and models of those enzymes.

I. Introduction

Oxygen-activating enzymes with mononuclear non-heme iron active sites participate in many metabolically important reactions that have environmental, pharmaceutical, and medical significance. For example, catechol dioxygenases and Rieske dioxygenases are involved in the degradation of aromatic molecules in the environment.[1] Lipoxygenases oxidize unsaturated fatty acids into precursors of leukotrienes and lipoxins and are potential targets for anti-inflammatory drugs.[2] Other enzymes like isopenicillin N synthase (IPNS)[3] and deacetoxycephalosporin C synthase,[4] an α-keto acid-dependent enzyme, are important in the biosynthesis of the β-lactam antibiotics such as penicillin and cephalosporin. Other α-keto acid-dependent enzymes participate in post-translational modification of amino acids in collagen[5] and blood-clotting factors.[6]

In the past decade, there has been an explosion of activity in this area,[7] and our understanding of these relatively unexplored metalloenzymes has significantly improved due to the greater availability of these enzymes from the use of molecular biology techniques, the consequent application of various spectroscopic techniques to elucidate the active site structure and the role of the metal center in catalysis, the development of functional synthetic models, and the solution of a number of protein crystal structures.

Crystal structures of four oxygen-activating enzymes with mononuclear non-heme iron active sites are now available: protocatechuate 3,4-dioxygenase (3,4-PCD, an intradiol-cleaving catechol dioxygenase),[8,9] 2,3-dihydroxybiphenyl 1,2-dioxygenase (BphC, an extradiol-cleaving catechol dioxygenase),[10,11] soybean lipoxygenase-1 (SLO-1),[12,13] and the Mn(II)-substituted isopenicillin N synthase (IPNS).[14] Figure 1 compares the metal sites of these four enzymes. There are two Tyr and two His ligands in 3,4-PCD, the only enzyme among the four that has an Fe(III)

S0009-2665(96)00039-8 CCC: $25.00

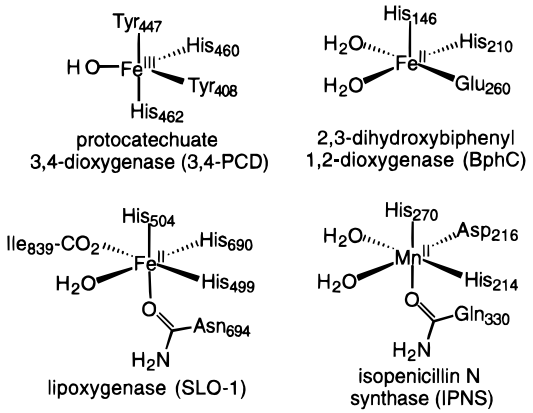

Figure 1. Metal coordination sites of the four crystallographically characterized mononuclear non-heme iron enzymes.

center in the as-isolated form. Presumably it is the presence of the tyrosine ligands that stabilizes the Fe(III) oxidation state; such ligands are absent in the other three enzymes, commensurate with their preference for Fe(II). Common among the latter three enzymes are two His ligands and one carboxylate arranged in a facial array that likely serves to hold the Fe(II) center in the active site. Interestingly, the SLO-1 and IPNS sites also contain an amide ligand derived from either Asn or Gln, representing a new feature of iron coordination chemistry in a protein. Finally, all four active sites have at least one coordination site that is vacant or occupied by solvent water and thus available for the binding of exogenous ligands such as substrate, cofactor, or O_2. This flexibility in coordination environment distinguishes these non-heme iron sites from those found in heme enzymes, where the only coordination site available for exogenous ligands is invariably designed for dioxygen or its analogues or derivatives. The greater variability of the iron coordination environments found in these enzymes increases the number of possible mechanisms by which dioxygen can be involved in substrate oxidation. In this review, we provide an up-to-date picture (briefly summarized in Table 1) of this fast-growing area and focus on recent developments in the enzymology of these structurally

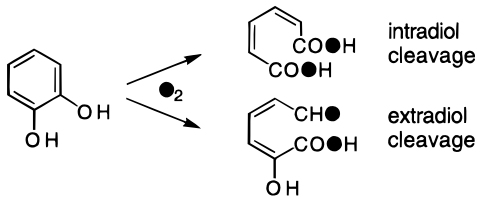

Figure 2. Modes of catechol cleavage.

characterized enzymes, i.e. the catechol dioxygenases, lipoxygenase, and isopenicillin N synthase, as well as that of the α-keto acid-dependent enzymes and the Rieske oxygenases.

II. Catechol Dioxygenases

The catechol dioxygenases serve as part of nature's strategy for degrading aromatic molecules in the environment;[1] they are found in soil bacteria and act in the last step of transforming aromatic precursors into aliphatic products (Figure 2). The intradiol-cleaving enzymes utilize Fe(III), while the extradiol-cleaving enzymes utilize Fe(II)[22,23] (and Mn(II) in a few cases[24−26]).

The intradiol-cleaving enzymes are represented by catechol 1,2-dioxygenase (1,2-CTD) and protocatechuate 3,4-dioxygenase (3,4-PCD). The combination of the rich spectroscopic properties of the iron(III) center and the availability of crystal structures for a number of enzyme complexes has provided a detailed picture of how these enzymes work. The crystal structure of 3,4-PCD from *Pseudomonas aeruginosa*[8,9] reveals a trigonal bipyramidal iron site with four endogenous protein ligands (Tyr408, Tyr447, His460, and His462) and a solvent-derived ligand (Figure 1). This active site picture corresponds remarkably well to that proposed earlier on the basis of spectroscopic studies.[23,27] Tyrosine ligation is indicated by the distinct burgundy red color ($\lambda_{max} \sim 460$ nm) of the enzymes and the appearance of characteristic resonance-enhanced Raman vibrations. Indeed, two tyrosine ν_{CO} bands at 1254 and 1266 cm^{-1} are observed, each with a different excitation profile, suggesting the presence of two distinct tyrosinates.[28−30] The

Table 1. Summary of Information about the Mononuclear Non-Heme Iron Enzymes

enzyme	requirement for activity	endogenous ligand set	coordination no. and geometry	functional models
catechol dioxygenase-intradiol cleavage	Fe(III) bound catechol	2 Tyr, 2 His	CN = 5 trigonal bipyramid	$[Fe(TPA)(DBC)]^{+}$ [15]
catechol dioxygenase-extradiol cleavage	Fe(II) bound catechol	2 His, Glu	CN = 5 square pyramid	$[Fe(TACN)(DBC)Cl]^{+}$ [16]
lipoxygenase	Fe(III)	3 His, Ile-CO_2^-, Asn	CN = 6 distorted octahedral	$[Fe(6\text{-}Me_3\text{-}TPA)(O_2CC_6H_5)]^{+}$ [17]
IPNS	Fe(II) bound ACV	2 His, Asp, Gln	CN = 6 distorted octahedral	$[Fe(TPA)(SPh)]^{+}$ [18]
α-keto acid-dependent enzymes	Fe(II) α-keto acid	NA[a]	NA[a]	$[Fe(6\text{-}Me_3\text{-}TPA)(BF)]^{+}$ [19] $Fe(Tp^{3,5-Me_2})(BF)$ [20]
Rieske oxygenases	Fe(II) Fe_2S_2 cluster NADH	NA[a]	NA[a]	NA[a]
bleomycin[b]	Fe(II) reducing agent	5 nitrogen ligands	CN = 5 square pyramid	$[Fe^{II}(PMA)]^{+}$ [21]

[a] Information is currently unavailable. [b] A natural product, used as an antitumor drug.

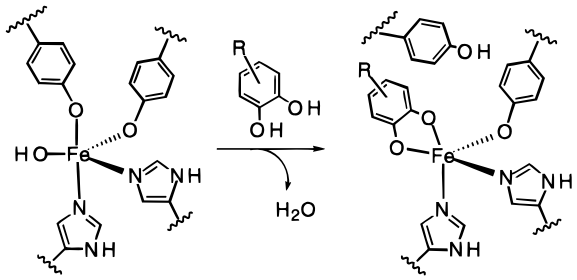

Figure 3. The proposed binding of substrate to protocatechuate 3,4-dioxygenase.

higher energy ν_{CO} is assigned to the more solvent-accessible axial Tyr447 due to its sensitivity to H_2O/D_2O exchange (6 cm^{-1} upshift) and the presence of exogenous ligands (up to a 40 cm^{-1} upshift).[30] Histidine ligation has been suggested from resonance Raman and EXAFS evidence.[30,31] The presence of a solvent-derived ligand was first indicated by the line broadening found in the EPR spectrum of the as-isolated enzyme from *Brevibacerium fuscum* when dissolved in $H_2{}^{17}O$.[32] Because the first shell EXAFS data requires three Fe−O bonds averaging 1.9 Å length, a distance which is typical of Fe(III)−phenolate and Fe(III)−hydroxide bonds, the solvent-derived ligand is thus identified as hydroxide.[33]

Substrate binding to the 3,4-PCD active site alters the spectroscopic properties of the Fe(III) center, but no redox chemistry occurs, as indicated by EPR and Mössbauer data.[34,35] There is a color change associated with the appearance of a long wavelength absorption that tails into the near IR region. Resonance Raman studies show that this new feature arises from a catecholate-to-Fe(III) charge transfer transition; furthermore, the vibrations observed are typical of a chelated catecholate dianion.[36,37] EPR studies of 3,4-PCD complexed with the substrate analogue 3,4-dihydroxyphenylacetate specifically ^{17}O-labeled at C-3 or C-4[38]and NMR studies of the 3,4-PCD−4-methylcatechol complex support this conclusion,[39] which is fully consistent with the strong affinity of Fe(III) for catecholate. In addition, the EPR studies demonstrate that the solvent-derived ligand is displaced upon substrate binding,[34] and the intensity of the X-ray absorption 1s→3d pre-edge transition indicates that the Fe(III) center remains five-coordinate in the PCD ES complex.[33] When interpreted together, the spectroscopic data suggest that substrate binding must result in the displacement of two ligands found in the as-isolated enzyme site, as shown in Figure 3. As the substrate most likely enters the active site with both its catecholic protons, these protons need to be absorbed upon binding to the Fe(III) center. Scrutiny of the active site environment revealed by the crystal structure shows that the only bases are the five that are coordinated to the Fe(III) center; therefore, the proposed ligand displacement is a plausible scenario. Further examination of the 3,4-PCD crystal structure suggests that the binding pocket would orient the substrate such that the plane of the ring would be more congruent with the trigonal axis than with the equatorial plane. Thus the substrate is proposed to displace the hydroxide and one of the axial ligands (Figure 3). The axial ligand that is displaced appears to be the axial tyrosine, as suggested by the loss of its characteristic ν_{CO} in the resonance Raman spectrum of the PCD ES complex.[40] Strong support for this notion derives from the crystal structure of 3,4-PCD complexed to 3-hydroxyisonicotinic acid *N*-oxide, a transition state analogue (Figure 4).[41] The struc-

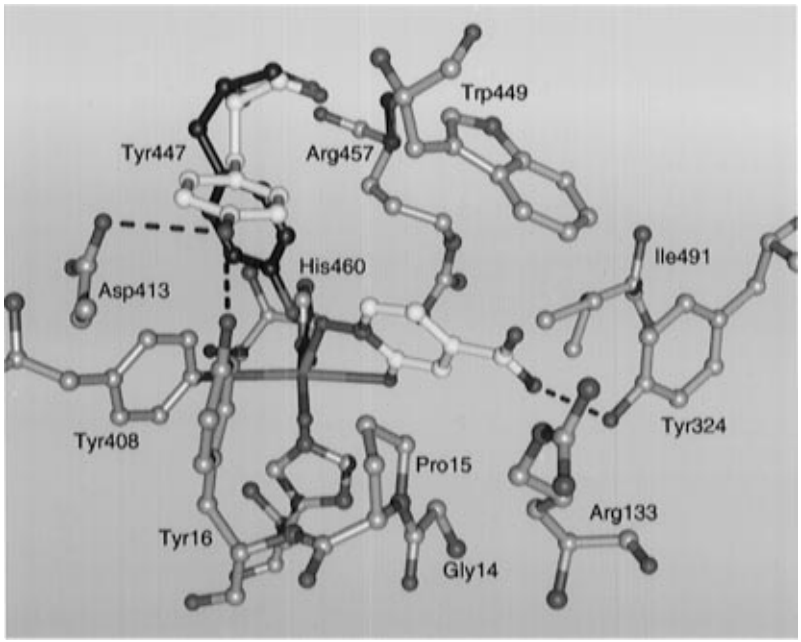

Figure 4. Changes in the active site of protocatechuate 3,4-dioxygenase upon binding the transition state analogue 3-hydroxyisonicotinic acid *N*-oxide derived from superimposing of the crystal structures of the active site of the enzyme and the enzyme−analogue complex. The only major change occurs with Tyr447, which is ligated to the Fe in the resting state of the enzyme (black representation of Tyr447) and is displaced when the analogue binds (yellow representation of Tyr447 and the analogue). The crystal structure also suggests that the displaced Tyr447 (in yellow) is appropriately positioned to hydrogen bond with Asp413 and Tyr16. The figure was kindly provided by A. M. Orville, D. H. Ohlendorf, and J. D. Lipscomb.

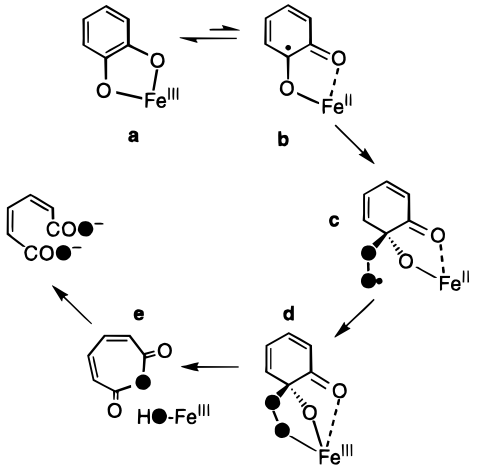

Figure 5. Proposed substrate activation mechanism for the intradiol-cleaving catechol dioxygenases.

ture shows the bidentate analogue occupying the coordination sites of the hydroxide and the axial tyrosine (the analogue and the displaced tyrosine are highlighted in yellow in Figure 4). As suggested by the spectroscopic data, the axial tyrosine is displaced upon protonation and swings away to hydrogen bond with other residues in the active site.

The prime mechanistic question of bioinorganic interest is the role of the iron center. Steady state kinetic studies show that the enzyme mechanism involves initial substrate binding followed by O_2 attack.[42] Given that the iron center in the enzyme−substrate complex is in the high-spin Fe(III) state,[32,35] it seems unlikely that O_2 binds to the iron center. This notion is supported by the observation that the ES complex does not react with the O_2 surrogate NO without prior reduction of the Fe(III) center.[43] Furthermore, studies on the reaction of the ES complex with O_2 reveal the involvement of intermediates that all retain the Fe(III) state.[35,44,45] The lack of spectroscopic evidence for the involvement of the Fe(II) oxidation state has led to the postulation of a substrate activation mechanism in which the coordination of catechol to the Fe(III) center activates the catechol for direct attack by O_2.[46]

The nature of this substrate activation has been clarified by the biomimetic studies of Que and coworkers[15,47,48] and is illustrated in Figure 5. This proposed mechanism is based on a study of a series of $[Fe^{III}(L)DBC]^+$ complexes where L is a tetradentate tripodal ligand. Three of these complexes have been structurally characterized and shown to have a six-coordinate environment with a chelated DBC^{2-} ligand (Figure 5a). All of the [Fe(L)DBC] complexes react with O_2 to yield the intradiol cleavage product, with the more Lewis acidic iron centers affording nearly quantitative conversion. Furthermore, the rate of reaction accelerates 3 orders of magnitude from L = NTA to L = TPA. The high reactivity of the TPA complex has been rationalized by the argument that increased Lewis acidity of the iron center enhances the covalency of the iron−catecholate interaction and enhances the semiquinone character of the bound DBC^{2-} (Figure 5b). This increased semiquinone character renders DBC^{2-} more prone to oxygen attack and accelerates the rate of oxidative cleavage.[15,47,48]

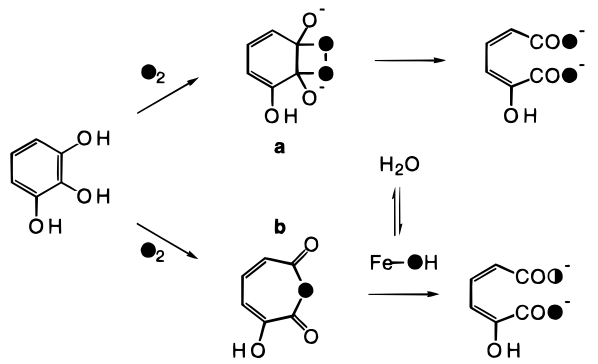

Figure 6. Two possible mechanisms for dioxygen incorporation in the intradiol cleavage of catechols.

The attack of O_2 on the activated substrate yields a transient alkylperoxy radical (Figure 5c) which combines with the equally short-lived Fe(II) center to generate an alkylperoxo−iron(III) species (Figure 5d). Support for the latter species has been obtained by Bianchini et al.[49−51] who have observed the formation of reversible O_2 adducts with Rh^{III}(triphos) and Ir^{III}(triphos) catecholate complexes. The crystal structure of the Ir adduct reveals that the bidentate catecholate has been transformed into the tridentate peroxy ligand analogous to Figure 5d. Decomposition of this peroxy adduct by a Criegee-type rearrangement to afford muconic anhydride (Figure 5e) has been demonstrated in biomimetic Fe(III) complexes.[15,47,48,52] That such an anhydride participates in the dioxygenase cycle (instead of the dioxetane proposed originally) is indicated by $^{18}O_2$-labeling studies of the reaction of 1,2-CTD with 1,2,3-trihydroxybenzene (Figure 6). The α-hydroxymuconic acid product derived therefrom shows some loss of ^{18}O label from one of the carboxylates.[53] This result excludes the dioxetane (Figure 6a) as an intermediate and requires that the incorporation of the elements of dioxygen occurs in two discrete steps, via the formation of an anhydride (Figure 6b) and its subsequent hydrolysis by an iron-bound hydroxide derived from O_2; solvent exchange with the Fe(III)−OH species would result in some loss of the second ^{18}O label.

The extradiol-cleaving catechol dioxygenases represent the more common cleavage pathway, but insight into these enzymes has lagged behind that of their intradiol-cleaving counterparts in part because of the fewer spectroscopic handles available to probe Fe(II) centers. This dearth of information has been alleviated in recent years by the application of a number of new spectroscopic approaches that have yielded the first details of the active sites of these enzymes. Of even more significance has been the solution of the first crystal structures of an extradiol-cleaving dioxygenase, 2,3-dihydroxybiphenyl 1,2-dioxygenase (BphC), by two independent groups.[10,11] Though the crystal structures reported are those of the active Fe(II) enzyme[10] and the inactive Fe(III) enzyme,[11] both reveal a square pyramidal iron site with three endogenous protein ligands (His146, His210, and Glu260) and two ligands derived from solvent (Figure 1). These results concur with the CD, MCD, and XAS data on catechol 2,3-dioxygenase (2,3-CTD) which support the presence of a five-coordinate Fe(II) site;[54,55] furthermore, the near IR transitions observed at 890 and 1811 nm in the CD and MCD

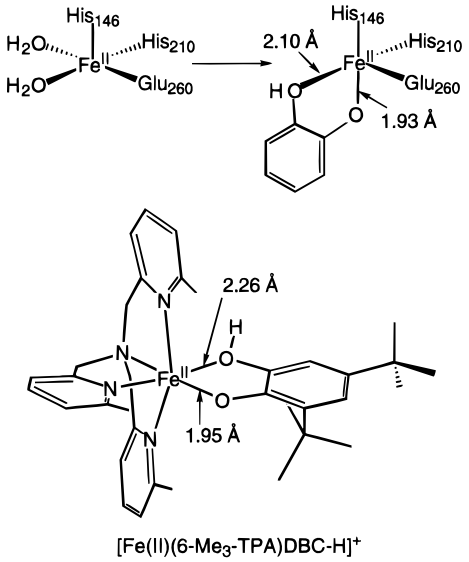

Figure 7. Structural changes accompanying substrate binding to an extradiol dioxygenase. Catechol chelates asymmetrically to the iron center, a binding mode found for a mono-anionic catecholate in [Fe(6-Me_3-TPA)DBC−H]$^+$.

studies have been interpreted to arise from a square pyramidal geometry.[54] Evidence for histidine coordination derives from the presence of outer shell features in the EXAFS spectrum of 2,3-CTD consistent with the presence of imidazole ligands[56] and from the observation of two solvent-exchangeable, paramagnetically shifted signals in the NMR spectrum of 2,2′,3-trihydroxybiphenyl dioxygenase at 62 and 74 ppm,[57] chemical shifts consistent with imidazole N−H's coordinated to high-spin Fe(II) centers. No spectroscopic evidence for the glutamate ligand has been obtained. Indirect evidence for at least one solvent-derived ligand has been obtained from the EPR spectra of the 2,3-CTD−NO and 4,5-PCD−NO complexes which are broadened in the presence of $H_2{}^{17}O$.[58]

Crystallographic studies of the BphC ES complex show that the substrate coordinates in a bidentate fashion (Figure 7).[11,59] One catecholate oxygen occupies the vacant sixth site in the as-isolated enzyme, while the other catecholate oxygen displaces the water ligand trans to His210. The other water ligand may also be lost. Spectroscopic (near IR CD, MCD, XAS) studies of 2,3-CTD are consistent with these results.[54,55] Furthermore ^{17}O broadening is observed in the EPR spectrum of the 4,5-PCD E•S•NO complex with substrate specifically ^{17}O-labeled at C-3 or C-4, but not for the complex in the presence of $H_2{}^{17}O$.[58,60] These observations indicate that the solvent-derived ligands are displaced upon formation of this complex; in addition, there must be three coordination sites available for the binding of substrate and NO (or O_2).

EXAFS studies on the 2,3-CTD−catechol complex have provided additional insight into the nature of the enzyme−substrate interaction.[55] While the fit to the first coordination sphere of the as-isolated enzyme consists of a single shell with five ligands at an average distance of 2.09 Å from the iron, the first sphere fit for the ES complex requires the inclusion of a scatterer at a significantly shorter distance (1.93 Å). This feature has been assigned to one of the catecholate oxygens by comparison to the structural data for the first example of a synthetic Fe(II)−catecholate complex, [Fe(6-Me_3-TPA)DBC−H]$^+$, which has Fe−$O_{catecholate}$ bonds of 1.95 and 2.26 Å (Figure 7).[61] The significant asymmetry in catechol binding in the synthetic complex stems from the presence of a bidentate but monoanionic catecholate, in contrast to the bidentate, dianionic catecholates commonly found among Fe(III) complexes. This difference is a result of the much weaker affinity of Fe(II) for catecholate, so the monoanionic ionization state is favored in the Fe(II) complex. The asymmetric bidentate coordination of substrate to the Fe(II) center in BphC is also supported by the crystal structure of the ES complex.[59]

Table 2 compares the salient properties of the two subclasses of catechol dioxygenases. The contrasting reactivities of the respective ES complexes toward NO provide an important clue to the distinct regiospecificities of these dioxygenases. The ES complexes of extradiol enzymes readily react with NO to form E•S•NO adducts, while those of intradiol enzymes do not react with NO unless the Fe(III) center is reduced prior to exposure to NO.[43] Thus the Fe(II) center in the extradiol-cleaving enzymes appears sterically and electronically poised to react with NO (and O_2 by inference); indeed, both the crystallographic and spectroscopic data show that there is a vacant site in the iron coordination sphere available for O_2 (or NO) binding. Interestingly, the coordination of the substrate appears to increase the affinity of the extradiol ES complex for NO,[58] probably by shifting the Fe(III/II) potential to more negative values.

A mechanism for extradiol cleavage has evolved from the above observations (Figure 8); such a mechanism must account for distinct regiospecificities of the intradiol and extradiol-cleaving enzymes. The first step appears to involve the binding of the substrate (Figure 8a) followed by the binding of O_2 to the Fe(II) center. Some electron transfer from metal to O_2 in the Fe(II)−O_2 species results in a superoxide-like moiety (Figure 8b) which gives the bound O_2 nucleophilic character. The bound O_2 attacks the carbon adjacent to the enediol unit in a Michael-type addition, to form a peroxy intermediate (Figure 8c) that decomposes by a Criegee-type rearrangement to the observed product (Figure 8d). This attack of a nucleophilic superoxide (vs an electrophilic dioxygen in the intradiol cleavage mechanism (Figure 5)) on the bound substrate serves as the cornerstone for the current proposed mechanism for extradiol

Table 2. Comparison of the Key Properties of the Catechol Dioxygenases

	intradiol-cleaving	extradiol-cleaving
metal center	Fe(III)	Fe(II)
endogenous ligands	2 Tyr, 2 His	1 Glu, 2 His
substrate binding mode	bidentate dianionic	bidentate monoanionic
reaction of ES complex with NO	requires prior reduction	immediate
proposed mechanism	electrophilic attack of bound substrate by O_2	nucleophilic attack of bound substrate by O_2^-

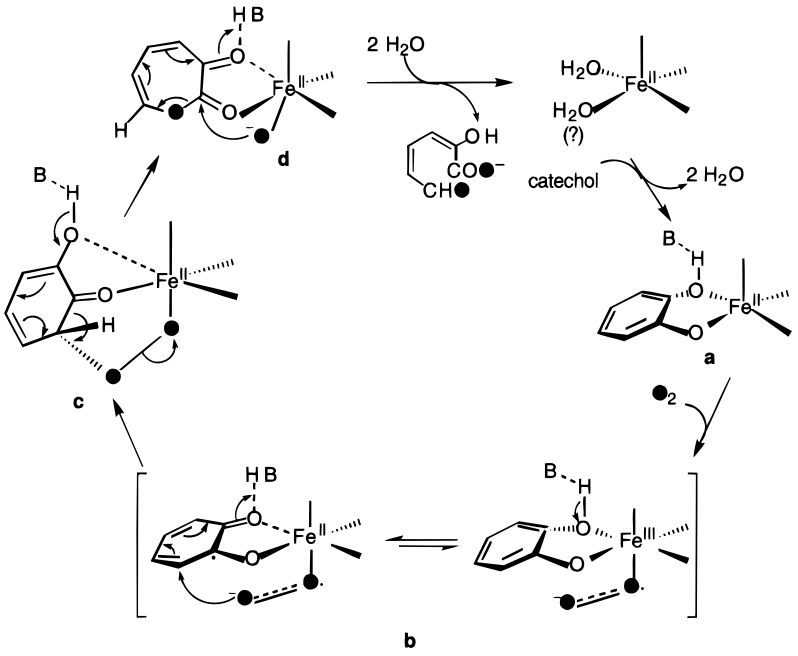

Figure 8. Proposed mechanism for the extradiol cleavage of catechol.

cleavage; it provides a very attractive rationale for the regiospecificity of dioxygen attack, as the bound substrate will undoubtedly have differing loci for nucleophilic and electrophilic attack.

While the proposed mechanism shown in Figure 8 is plausible, much work remains to be done to substantiate the individual steps. Thus far, reaction conditions have not been identified that would allow some of the steps to be kinetically resolved. In particular, the key nucleophilic attack by superoxide may be substantiated if such an attack is found to be accelerated by the presence of electron-withdrawing groups on the catechol ring. (In rapid kinetic studies of the intradiol-cleaving enzymes, the attack of O_2 on the substrate is found to be accelerated by electron-donating groups.[44,62]) As with the intradiol enzymes, mechanistic insights may also derive from appropriate functional models. Dei et al.[16] have reported that $[Fe(TACN)(DBC)Cl]^+$ affords nearly exclusive extradiol cleavage (35% yield) upon exposure to O_2; building on these observations, Ito and Que[63] have found conditions under which extradiol cleavage approaches quantitative conversion. Though this model is an iron(III) complex instead of an iron(II) species as in the enzymes, the availability of such a complex opens the door for systematic studies on the electronic factors affecting this reaction.

Evidence for the participation of the lactone species (Figure 8d) that results from O−O cleavage has recently been obtained for 3-(2′,3′-dihydroxyphenyl)propionate 1′,2′-dioxygenase (MhpB) (Figure 9).[64] When $H_2{}^{18}O$ is introduced into the solvent, the carboxylate group of the extradiol cleavage product becomes labeled; conversely, the extradiol cleavage product derived from $^{18}O_2$ shows some loss of label (Figure 9). Furthermore, a lactone analogue (Figure 9) is also hydrolyzed when treated with MhpB. These experiments demonstrate that solvent can access the active site during the reaction and exchange with the Fe(II)−OH moiety needed to open the lactone ring. Further developments in our understanding of these

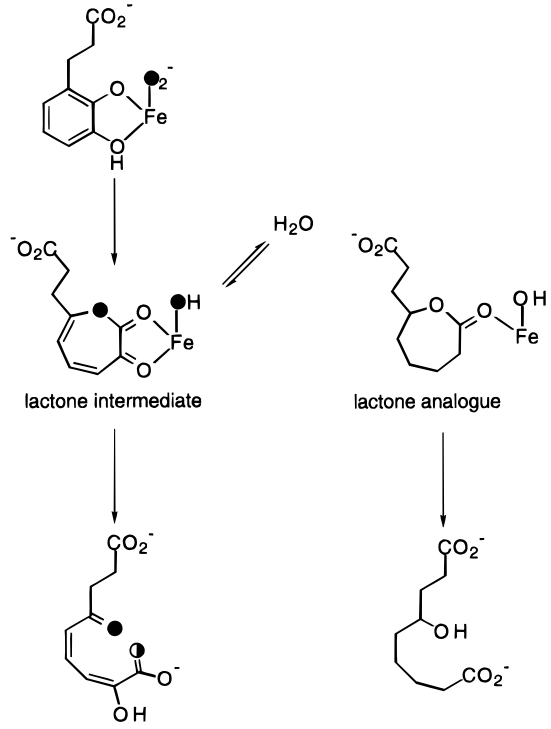

Figure 9. Evidence for lactone intermediate in the extradiol cleavage in MhpB.

enzymes are likely in the near future, as efforts mature in light of these recent exciting results.

Two other enzymes deserve mention in the context of the extradiol-cleaving dioxygenases. The first is gentisate 1,2-dioxygenase (1,2-GTD), which catalyzes the cleavage of the C1−C2 bond of 2,5-dihydroxybenzoate[65] (Figure 10). This enzyme behaves like an extradiol-cleaving enzyme, in that it requires Fe(II) for activity and binds NO more tightly in the presence of substrate. ^{17}O-Labeling of the substrate shows that it coordinates to the metal center via the carboxylate and the 2−OH group. A mechanism analogous to that for an extradiol enzyme has been

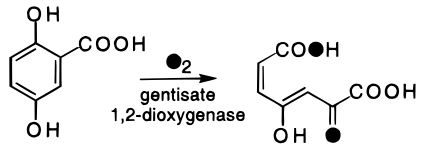

Figure 10. Reaction catalyzed by gentisate 1,2-dioxygenase.

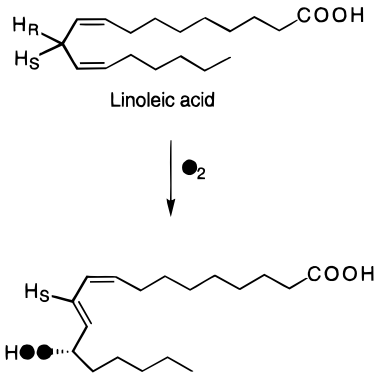

Figure 11. Enzymatic reaction of soybean lipoxygenase-1.

proposed.[65] The second is 3,4-dihydroxyphenylacetate 2,3-dioxygenase (MndD) from *Arthrobacter globiformis*, which is an extradiol-cleaving enzyme that requires Mn(II) instead of Fe(II).[24−26] However, sequence analysis has shown that it belongs to the super family of extradiol dioxygenases;[25] indeed, the three amino acid residues identified as ligands in the BphC structure are strictly conserved within this super family, including MndD. The Mn(II) center has spectroscopic properties very different from that of Fe(II) and may provide new avenues for exploring the role of the metal center in these enzymes.[26]

III. Lipoxygenases

Lipoxygenases, which catalyze the oxidation of unsaturated fatty acids containing the *cis*,*cis*-1,4-pentadiene moiety to the corresponding 1-hydroperoxy-*trans*,*cis*-2,4-diene, are widely found among plants and animals.[2] The mammalian enzymes typically act on arachidonic acid to produce hydroperoxides that are precursors to leukotrienes and lipoxins, compounds that have been implicated as potential mediators of inflammation. For this reason, many studies have focused on finding inhibitors of mammalian lipoxygenases as anti-inflammatory drugs. Linoleic acid is the substrate for the plant lipoxygenases; in this case, a C-11 hydrogen (H_R) is stereospecifically removed and the C-13-(*S*)-OOH is stereospecifically formed (Figure 11). The role of the product hydroperoxide is not known in plant metabolism, although it has been proposed to be linked to plant growth and development and the biosynthesis of regulatory molecules.[66,67] Currently, the majority of information about these enzymes has come from studies of soybean lipoxygenase-1 (SLO-1), due to its ease of purification, though the recent availability of cloned and overexpressed mammalian 5-lipoxygenase has begun to allow comparisons between the plant and mammalian enzymes to be made.[68]

Sequence analysis of 14 lipoxygenases from both plant and animal sources reveals significant homology, in particular six conserved histidine residues. Site-directed mutagenesis studies on these six histidines in SLO-1 indicate that three of these histidines (499, 504, and 690) are possible iron-binding ligands.[69,70] Furthermore, UV/vis studies of the catecholate complexes of Fe^{III}SLO-1 predict that the Fe center is bound to three neutral ligands, possibly His residues, and one carboxylate.[71] The ligand set of three histidines and one carboxylate has recently been confirmed by two reported crystal structures of Fe^{II}(SLO-1) (Figure 1).[12,13] In both crystal structures the carboxylate ligand derives from the carboxy terminal residue Ile839. A fifth endogenous ligand, Asn694, is also identified in one of the crystal structures.[13] This residue is conserved in most lipoxygenases except for the 15-lipoxygenases from human and rabbit, where a His residue replaces the Asn residue. A recent site-directed mutagenesis study of the corresponding Asn713 of soybean lipoxygenase-3 suggests that the Asn is not required for iron binding but is important for catalysis.[72]

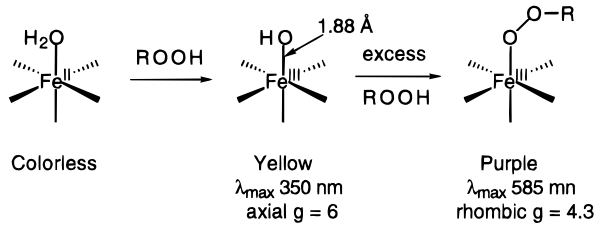

Figure 12. The three spectroscopically characterized species in lipoxygenase-1.

As-isolated, SLO-1 is colorless and the iron is in the high-spin Fe(II) state. This form appears to be inactive, and full enzymatic activity is elicited only after the center is oxidized to the high-spin Fe(III) state. Magnetic circular dichroism (MCD) studies of Fe^{II}SLO-1 indicate that the iron center exists as a 40/60 mixture of five- and six-coordinate species.[73] Though not observed in the crystal structures, a solvent molecule is likely to occupy the sixth coordination site in SLO-1. This ligand is displaced when the Fe(II) enzyme is exposed to NO to form an $S = 3/2$ Fe−NO adduct.[74]

The high-spin Fe^{III}SLO-1 is yellow (λ_{max} 350 nm) and associated with an axial EPR ($g = 6$) spectrum.[75] Interestingly, the only known oxidant to afford this active species is the product hydroperoxide, which suggests that the lipoxygenase reaction may be initiated by the autoxidation of linoleic acid. Indeed, a lag phase is observed in the catalytic activity when starting with the Fe(II) enzyme. XANES and MCD studies on Fe^{III}SLO-1 indicate that the Fe(III) center is six-coordinate.[76−78] The five endogenous ligands identified in the crystal structure are presumably bound, and the sixth ligand is derived from solvent as evidenced by the broadening of the axial Fe(III) EPR signal in the presence of $H^{17}O$.[79] Also, EXAFS studies of yellow SLO-1 show the presence of a short (1.88 Å) bond, which has been assigned to a hydroxide ligand (Figure 12).[76]

Yellow SLO-1 converts to a transient purple species in the presence of excess hydroperoxide (Figure 12).[80] The structure of this purple species has not been determined, although it has been postulated as an intermediate during the catalytic cycle. Spectro-

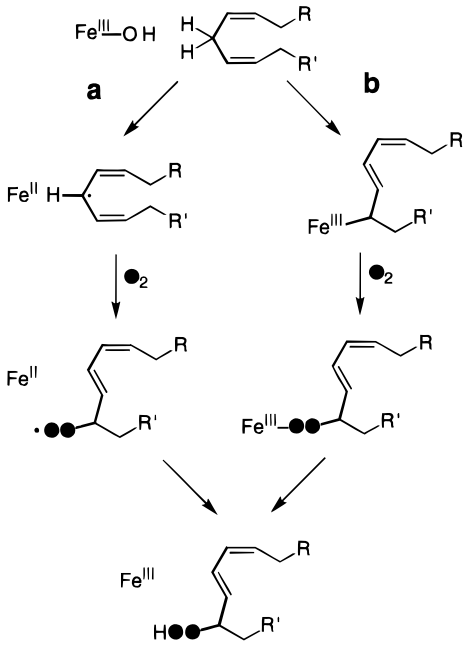

Figure 13. Proposed enzymatic mechanism for lipoxygenase.

scopic characterization of this transient purple species shows a λ_{max} at 585 nm and a rhombic, high-spin Fe(III) EPR signal at $g = 4.3$. Insight into the nature of this species has been obtained from model studies. Zang et al.[17] showed that the visible spectral changes associated with the lipoxygenase cycle can be modeled with $[Fe^{II}(6\text{-}Me_3\text{-}TPA)O_2CC_6H_5]^+$. This complex reacts stoichiometrically with an alkyl hydroperoxide to form a high-spin Fe(III) species which subsequently converts to a pink species with excess alkyl hydroperoxide. Resonance Raman studies demonstrate that the pink chromophore (λ_{max} 508 nm) derives from an alkylperoxo-to-Fe(III) charge transfer transition. The similarity in the spectral changes in the presence of excess ROOH suggests that the purple lipoxygenase intermediate may also be an Fe(III)−alkylperoxo species.

Mammalian lipoxygenases also undergo similar spectral changes when treated with product hydroperoxide. Like SLO-1, human 5-lipoxygenase affords a yellow, high-spin Fe(III) species (λ_{max} 350 nm) with an axial EPR spectrum.[81] In contrast, rabbit and human 15-lipoxygenases give rise to a yellow, high-spin Fe(III) form with a rhombic EPR spectrum which is converted to an axial EPR signal in the purple form.[82] This reversal in EPR properties relative to those of SLO-1 has been ascribed to the substitution of the Asn ligand to a His residue, as indicated by a sequence comparison between the 5- and 15-lipoxygenases.[82] The replacement of the weaker field Asn residue with the more basic His residue may account for the observed changes in the EPR spectra.

The details of how lipoxygenase oxidizes fatty acids have been a matter of debate.[2] Discussion centers around the role of the Fe(III) center in the catalytic mechanism. One mechanism (Figure 13a) proposes that the Fe(III) center reacts with linoleic acid to abstract the C-11 hydrogen, generating an Fe(II) center and the pentadienyl radical, which then reacts with O_2.[83,84] The alternative mechanism (Figure 13b) involves the abstraction of the substrate C-11 proton to form an organoiron(III) intermediate, which then reacts with O_2.[85] The reaction of either the Fe(II)−substrate radical or the organoiron(III) species with O_2 affords the Fe(III) enzyme and the product hydroperoxide. The stereospecificity of the lipoxygenase reaction makes the organoiron mechanism quite attractive and argues against the involvement of a substrate free radical which may readily lose its stereochemistry.[85] However, the observed reduction of the Fe(III) center by linoleic acid in the absence of O_2 to produce a linoleyl radical intermediate would appear to support the substrate radical mechanism.[84,86,87]

A key step in either proposed mechanism is the cleavage of the substrate C−H bond. Indeed, this step is known to proceed with a significant kinetic isotope effect, showing that it is involved in the rate determining step of the reaction. k_H/k_D values in the range of 30 for both k_{cat} and k_{cat}/K_m have been reported in two independent studies, and tunneling effects have been invoked to explain these very large values.[88−90] The active agent involved in this C−H bond cleavage is currently unclear. For the organoiron mechanism, an active site base strong enough to pull off the doubly allylic proton of a 1,4-pentadiene unit is required; it seems unlikely that the Fe(III)−OH moiety in the active enzyme would be sufficiently basic to fulfill this function. On the other hand, the substrate radical mechanism may involve an outer sphere reaction between the Fe(III) center and the substrate. That such a mechanism has merit has been demonstrated recently by Bill et al.[91] in the oxidation of 1,4-cyclohexadienes to arenes by $[Fe(phen)_3]^{3+}$ complexes. They demonstrate a correlation between the rate of oxidation and the redox properties of the iron complex and the diene substrate. The two driving forces for the model reaction are the high potentials (ca. 1.2 V vs NHE) of the iron complexes and the conformational constraints imposed on the diene unit by the ring which can provide maximum π interaction when the hydrogen is abstracted. Thus the enzyme active site could in principle provide the conformational constraints required to enhance the formation of the pentadienyl radical, and the oxidation could occur provided the redox potential of the iron site is high enough. However, Nelson has estimated the potential of the iron site in lipoxygenase to be approximately 600 mV vs NHE,[92] which may be too low of a driving force for a pure outer sphere reaction (for 1,4-cyclohexadiene, $E°_{1/2} = +1.1$ V vs NHE[93]).

We propose a variation of the outer sphere oxidation mechanism by drawing an analogy with the alkane oxidation mechanisms of cytochrome P450 and related alkane monooxygenases. These enzymes utilize a metal−oxo species to couple C−H bond cleavage with a reduction of the iron center, i.e.

$$M^{(n+1)+}{=}O + R{-}H \rightarrow M^{n+}{-}OH + R^{\bullet}$$

As elegantly argued by Mayer in his papers on alkane oxidations by metal−oxo species,[94,95] the three factors that affect this reaction are the redox potential of the metal center, the strength of the C−H bond

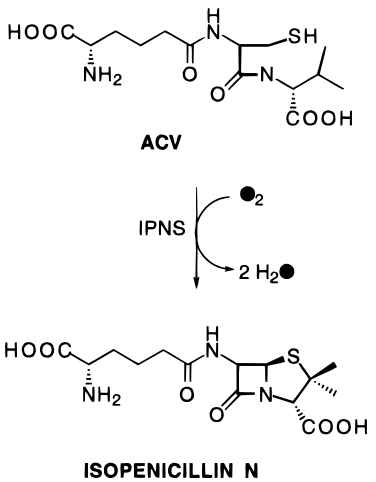

Figure 14. Reaction catalyzed by isopenicillin N synthase.

being broken, and the strength of the O−H bond being formed. The last provides additional driving force for the reaction when compared to the purely outer sphere mechanism discussed above. Since the C−H bond cleaved in lipoxygenase belongs to a pentadiene unit and would thus be about 25 kcal/mol ($D_{C-H} = 76 \pm 3$ kcal/mol)[96] weaker than those cleaved by alkane monooxygenases, the higher potentials associated with the Fe(IV) oxidation state utilized by the alkane monooxygenases may not be required to carry out this reaction. The moderately high potential of the Fe(III)−OH center of lipoxygenase and its conversion to an Fe(II)−OH_2 center may be sufficient to cleave the substrate C−H bond. Some inkling that such a mechanism may work has been recently reported by Zang et al.,[97] who demonstrated the following reaction:

$$[Fe^{III}_2(\mu\text{-O})(\mu\text{-OH})(6\text{-Me}_3\text{-TPA})_2]^{3+} + \text{1,4-cyclohexadiene} + H^+ \xrightarrow{CH_3CN} \text{benzene} + 2[Fe^{II}(6\text{-Me}_3\text{-TPA})(CH_3CN)_2]^{2+} + 2H_2O$$

Further work needs to be carried out to support this hypothesis.

IV. Isopenicillin N Synthase

The importance of penicillin- and cephalosporin-related antibiotics in medicine has provided the impetus for understanding the mechanism of formation of these compounds. It is now known that the key steps in the biosynthesis of these antibiotics in some microorganisms are the oxidative ring closure reactions of δ-(L-α-aminoadipoyl)-L-cysteinyl-D-valine (ACV) to form isopenicillin N, the precursor of penicillins and cephalosporins (Figure 14).[3] The enzyme responsible for this transformation is isopenicillin N synthase (IPNS), which requires Fe(II) and O_2 for reactivity. The overall reaction utilizes the full oxidative potential of O_2, giving 2 equiv of H_2O for each O_2 and transforming ACV to isopenicillin N. Since both oxygen atoms of O_2 are converted to H_2O, these enzymes are technically oxidases, and the four electrons required for this reduction originate from ACV.

The crystal structure of the Mn(II)-substituted IPNS from *Aspergillus nidulans* has been recently reported showing a six-coordinate Mn ion bound to the enzyme via four endogenous protein ligands (two histidines, an aspartate, and a glutamine) with the remaining coordination sites occupied by two H_2O molecules (Figure 1).[14] This crystal structure confirms and enhances the ligand information derived earlier from biochemical and spectroscopic studies. From sequence comparisons, there are seven conserved His residues in IPNS, but only two are found to be essential for activity, as indicated by site-directed mutagenesis experiments.[14,98,99] These two His residues are observed in ESEEM studies of Cu^{II}-IPNS (based on the observation of ^{14}N signals typical of the distal nitrogen of imidazole)[100] and in the NMR spectra of Fe^{II}IPNS and Co^{II}IPNS (based on the appearance of solvent-exchangeable N−H resonances observed in a region typical of paramagnetically shifted imidazole N−H protons).[101] Though the NMR studies suggest that there are three His ligands, the crystal structure indicates that one of the paramagnetically shifted N−H resonances observed must arise from a residue other than His, perhaps from the Gln ligand. Due to its unexpected occurrence in IPNS and the lack of diagnostic spectroscopic probes, the glutamine ligand was not identified prior to the crystal structure. Aspartate ligation has been identified from NMR studies of Co^{II}IPNS and Co^{II}IPNS−ACV on the basis of NOE connections among the three Asp C_α and C_β protons in the appropriate chemical shift region.[101] The presence of at least one solvent-derived ligand is indicated by the broadening of the $S = 3/2$ EPR signals of Fe^{II}IPNS−NO upon introduction of $H_2{}^{17}O$.[102]

With the crystallographic determination of the active site environment in IPNS, the catalytic mechanism becomes the primary question to be answered. On the basis of reactivity studies by Baldwin et al.[3] using isotopically labeled substrates and a host of substrate analogues, a proposed reaction mechanism is given in Figure 15. The initial steps of the reaction are proposed to be the consecutive binding of ACV and O_2 to the Fe(II) center (Figure 15a). The binding of the ACV thiolate to Fe^{II}IPNS is indicated by a number of spectroscopic studies. First, Mössbauer spectroscopy shows that the addition of ACV to Fe^{II}-IPNS causes a decrease in the isomer shift of the Fe(II) center from 1.2 to 1.0 mm/s, suggesting the formation of a more covalent Fe(II)−ligand environment.[102] Secondly, UV/vis studies of Cu^{II}IPNS show the appearance of an intense band at 390 nm upon addition of ACV that is associated with a thiolate-to-Cu(II) charge transfer transition found for type II copper proteins.[103] Finally, EXAFS analysis of the Fe^{II}IPNS−ACV complex indicates the presence of a sulfur scatterer at ca. 2.3 Å, which is a distance typical of Fe(II)−thiolate ligation.[104,105] From an examination of the structure of the Mn^{II}IPNS, it is likely that the ACV thiolate displaces one of the solvent-derived ligands. Since the enzyme becomes O_2-sensitive only after addition of ACV, it would appear that the coordination of the ACV thiolate to the Fe(II) center causes a decrease in the Fe(III/II) redox potential, thereby priming the Fe(II) center for its reaction with O_2.

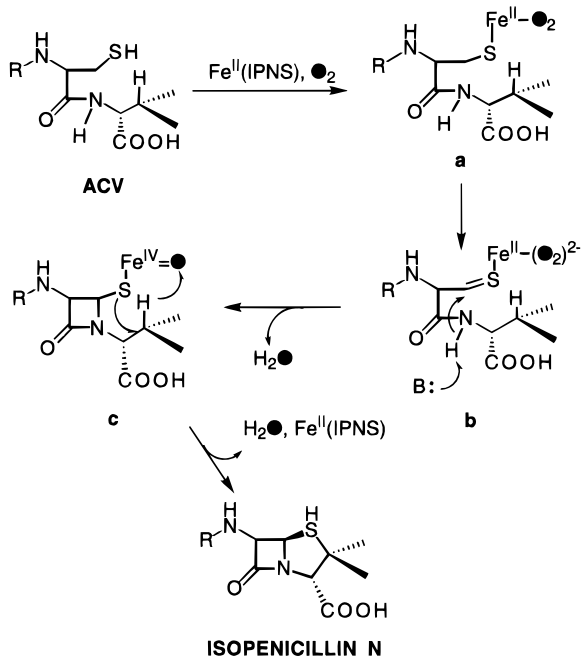

Figure 15. The proposed mechanism of isopenicillin N synthase.

Unfortunately, spectroscopic evidence for an Fe^{II}-IPNS−ACV−O_2 adduct has not yet been obtained because of the reactivity of this ternary complex. However, NO serves as a useful O_2 analogue and spectroscopic studies of the Fe^{II}IPNS−ACV−NO complex have provided important insights. NO binding to Fe^{II}IPNS−ACV is indicated by the appearance of an $S = 3/2$ EPR spectrum[102] and the requirement for a 1.76 Å scatterer due to the Fe−NO bond in the EXAFS fit of Fe^{II}IPNS−ACV−NO.[104] The ligation of the ACV thiolate was evidenced by the larger rhombicity of its EPR spectrum ($g = 4.22$, 3.81, and 1.99 with $E/D = 0.035$) relative to that of Fe^{II}IPNS−NO ($g = 4.09$, 3.95, and 2.0 with $E/D = 0.015$) and the appearance of visible bands at 508 and 720 nm which are red-shifted relative to those observed for Fe^{II}-IPNS−NO and Fe^{II}IPNS−ASerV−NO. Furthermore, EXAFS analysis of Fe^{II}IPNS−ACV−NO requires the presence of an Fe−S scatterer at 2.3 Å. The visible and EPR spectroscopic properties observed for $[Fe^{II}$-$(TPA)(SC_6H_2$-2,4,6-$Me_3)NO]^+$ derived from exposure of $[Fe^{II}(TPA)(SC_6H_2$-2,4,6-$Me_3)]^+$ to NO support this interpretation.[18] Lastly, there is a solvent-derived ligand on the iron center of Fe^{II}IPNS−ACV−NO, as the EPR spectrum is broadened by the introduction of $H_2{}^{17}O$.[102] Thus the above data indicate that three coordination sites on the iron center of Fe^{II}IPNS−ACV−NO are occupied by exogenous ligands.

With four endogenous ligands identified in the structure of Mn^{II}IPNS, NO binding to Fe^{II}IPNS−ACV must displace one of these. The displacement of one of these ligands is supported by the loss of the diagnostic signals for the Asp ligand and one of the N−H resonances in the NMR spectra of Fe^{II}IPNS−NO and Fe^{II}IPNS−ACV−NO.[101] Which ligand is displaced is currently unclear, although the difference in charge between a carboxylate and an amide makes the displacement of Gln by NO seem more likely. On the other hand, 3,4-PCD provides the precedence for the displacement of an anionic ligand

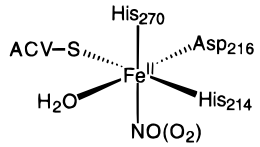

Figure 16. Proposed structure for the ternary Fe^{II}IPNS−ACV−NO (O_2) complex.

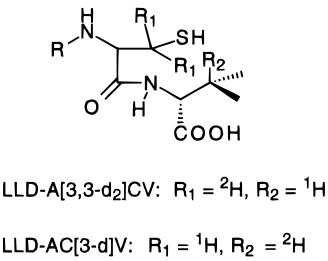

Figure 17. Deuterated substrates for isopenicillin N synthase used to test a two-step mechanism involving consecutive ring formation steps.

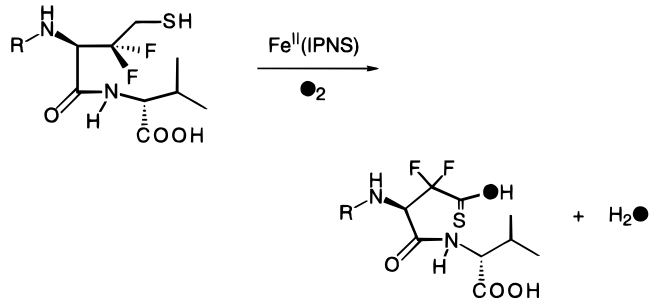

Figure 18. The reaction of isopenicillin N synthase and a substrate analogue.

(Tyr) over a neutral one (His) in the formation of its substrate complex (see Figure 4). Taking into consideration the spectroscopic data for Fe^{II}IPNS−ACV−NO and the crystal structure of Mn^{II}IPNS, Fe^{II}IPNS−ACV−O_2 is proposed to have the structure shown in Figure 16.

What happens after ACV and O_2 binding is currently unclear since no intermediates have yet been characterized. Deuterium labeling studies by Baldwin et al.[3,106] support a multistep mechanism in which the formation of isopenicillin N occurs via sequential ring closure steps to form first the β-lactam ring and then the thiazolidine ring. Competition experiments with LLD−ACV and LLD−A[3,3-D_2]CV (Figure 17) show that IPNS reacts preferentially with LLD−ACV, suggesting that the removal of the Cys-α-C-H hydrogen is at least partially rate determining.[106] Conversely, no preference between the two substrates is detected when similar competitive studies with LLD−ACV and LLD−AC[3-D]V are carried out; i.e., the disappearance of LLD−ACV and LLD−AC[3-D]V occurs at equal rates. If the reaction occurs through an one-step mechanism, then deuteration of either Cys α-C or Val α-C should slow down the enzyme reaction since the cleavage of both the Cys α-C−H and Val α-C−H bonds would occur during the ring formation steps. The observation that only the deuteration at the Cys α-C affects the rate of reaction suggests that the cleavage of the Cys α-C−H bond, and therefore the formation of the β-lactam ring, is irreversible and occurs prior to the cleavage of the Val α-C−H bond.

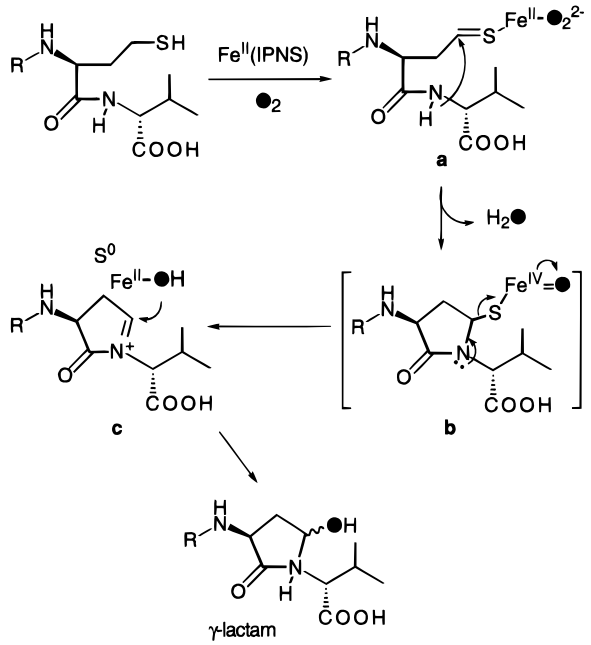

Figure 19. Proposed reaction mechanism for the formation of a hydroxylated γ-lactam from the reaction of isopenicillin N synthase with the homocysteine analogue of ACV.

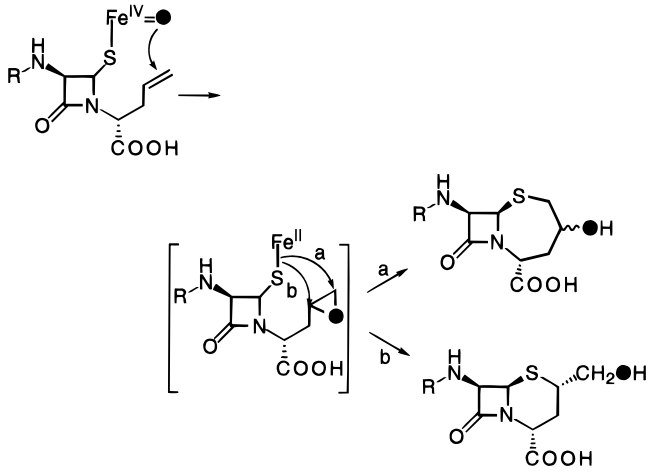

Figure 20. Evidence for an epoxide intermediate in the reaction of isopenicillin N synthase with an allylglycyl analogue of ACV.

The β-lactam ring formation step involves the initial oxidation of the Cys thiol of ACV by two electrons to give a thioaldehyde or some equivalent moiety, while O_2 is reduced by two electrons to the peroxide (Figure 15b). Support for the initial oxidation of the thiol comes from the reaction of Fe(IPNS) and an ACV analogue with a difluorinated homocysteine which gives the corresponding thioacid as the only product (Figure 18).[107]

Following the oxidation of the thiol, nucleophilic attack of the valinyl peptide nitrogen on the Cys β-carbon then forms the β-lactam ring and regenerates the thiolate. Products in which only the β-lactam ring is formed have not been observed; however, γ-lactams from the homocysteine analogue have been isolated.[108] In this reaction, the thiolate is oxidized to elemental sulfur, and oxygen is incorporated into the γ-lactam via a proposed mechanism shown in Figure 19. The mechanism involves the initial oxidation of the thiol to give a thioaldehyde and a peroxide, which are both bound to the Fe (Figure 19a). Attack of the Val amine on the Cys α-C gives the monocyclic intermediate (Figure 19b) that rapidly collapses to break the C−S bond, to give atomic sulfur, an iminium ion, and an Fe−OH species (Figure 19c). Attack of the bound OH^- on the iminium species then gives the hydroxy γ-lactam that has been isolated. The fact that reactions occur at the Cys residue without transforming the Val residue also supports the notion that the β-lactam ring forms first.

The subsequent step to form the thiazolidine ring is proposed to involve a high valent iron−oxo species derived from the heterolysis of an iron(II)−peroxo intermediate (Figure 15c). The participation of the iron−oxo species is suggested by the reaction with an allylglycyl analogue which gives products that may arise from the nucleophilic attack of the thiolate on an intermediate epoxide. This epoxide could be derived from the attack on the double bond by an iron(IV)−oxo moiety (Figure 20), analogous to the reaction of cytochrome P450.[109] In forming the thiazolidine ring from the natural substrate, this iron−oxo species abstracts the valinyl β-H to form an Fe(III)−OH and an alkyl radical, a step reminiscent of the cytochrome P450-catalyzed alkane hydroxylation mechanism.[110] When a cyclopropyl group

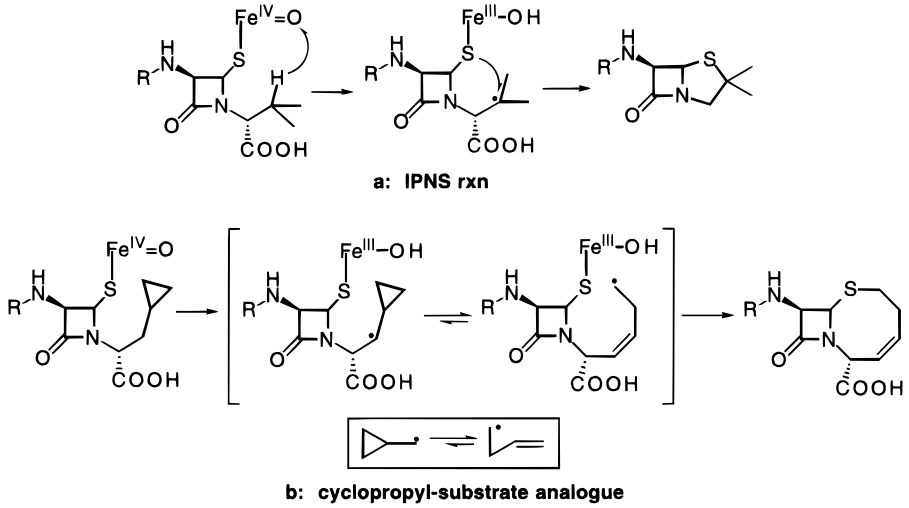

Figure 21. Evidence for the formation of an alkyl radical in the isopenicillin N synthase reaction.

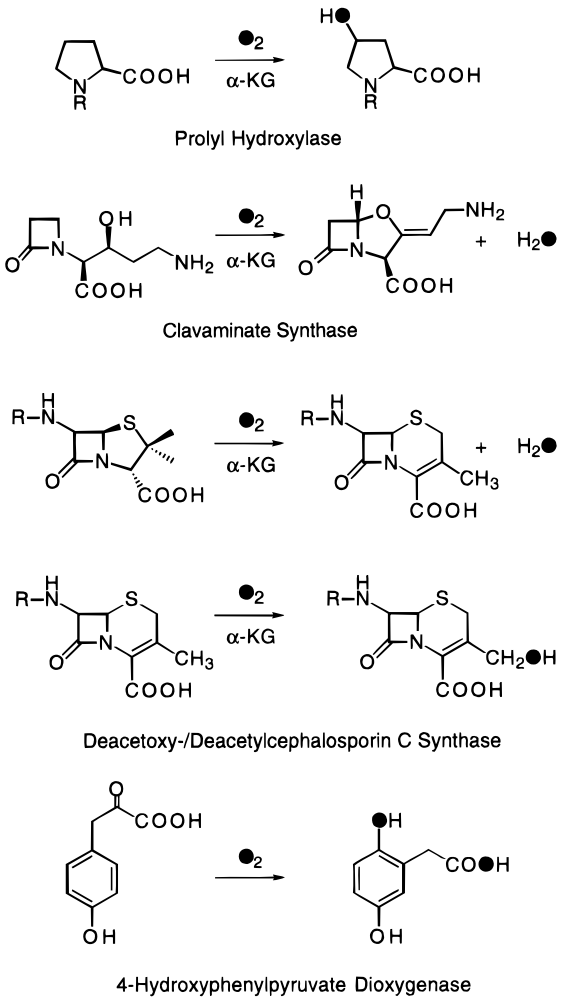

Figure 22. Examples of α-keto acid-dependent dioxygenases.

is introduced into the valinyl residue, products derived from the rearrangement of a cyclopropylcarbinyl radical are observed, in support of an alkyl radical intermediate (Figure 21b).[111] However, in the cytochrome P450 mechanism, the alkyl radical subsequently combines with the coordinated OH to give the hydroxylated product. In the IPNS mechanism, the nascent alkyl radical combines with the coordinated thiolate instead of the hydroxide to form the thiazolidine ring. A similar preference for an oxidative transfer of a ligand other than hydroxide has been demonstrated by the efficient conversion (70−80% yield) of cyclohexane to halocyclohexanes by the reaction of $[Fe(TPA)X_2]^+$ (X = Cl, Br) and a stoichiometric amount of ^{t}BuOOH, where the transfer of the halogen is highly favored over the hydroxide.[112,113]

V. α-Keto Acid-Dependent Enzymes

The α-keto acid-dependent enzymes are distinguished from other non-heme iron enzymes by the requirement of an α-keto acid cofactor as well as Fe(II) and O_2 for reactivity. They now constitute a large class of enzymes which are essential in the biosynthesis of many biological compounds.[5,114,115] Examples of these enzymes (Figure 22) include prolyl hydroxylase, which hydroxylates specific prolyl residues of the collagen chain;[5] clavaminate synthase, a key enzyme in the synthesis of clavulanic acid, an

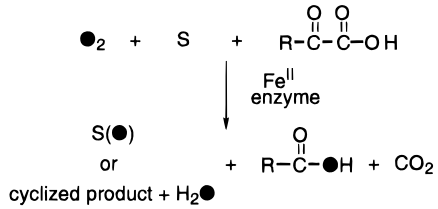

Figure 23. General reactions catalyzed by α-keto acid-dependent enzymes.

important β-lactamase inhibitor;[116] deacetoxycephalosporin C synthase, which catalyzes the ring expansion of isopenicillin N to deacetoxycephalosporin (DAOC) and the subsequent hydroxylation of DAOC to deactylcephalosporin C (DAC);[4,117] and 4-hydroxyphenylpyruvate dioxygenase, which converts 4-hydroxyphenylpyruvate to homogentisate, an important reaction in the tyrosine catabolic pathway.[118,119] In general, the reactions catalyzed by these enzymes involve the oxidation of an unactivated C−H bond to give either hydroxylated products as in prolyl hydroxylase or oxidative cyclization products as in clavaminate synthase. Deacetoxycephalosporin C synthase is particularly interesting because this enzyme has been shown to catalyze both the hydroxylation and cyclization reactions in its enzymatic activity.[4] For both types of reactions, the α-keto acid loses CO_2 and the keto functional group is oxidized to a carboxylate with one of the carboxylate oxygens coming from O_2 (Figure 23). The other oxygen from O_2 is either incorporated into the hydroxylated product in the hydroxylation reaction or converted into H_2O in the cyclization reaction. With 4-hydroxyphenylpyruvate dioxygenase,[119] the α-keto acid is attached to the substrate such that the resulting product comes from an intramolecular hydroxylation where both oxygens of O_2 are incorporated into the product, homogentisate (Figure 22).

In general, these enzymes require 1 equiv of Fe(II), an α-keto acid (usually α-ketoglutarate), and ascorbate for full activity. Substitution with other divalent metal ions (Zn(II), Cu(II), Mn(II), Co(II), Mg(II), and Ni(II)) results in the complete loss of enzymatic activity, which is attributed to competitive binding of these ions at the active site.[120−122] Similarly, substitution of α-ketoglutarate (α-KG) with other α-keto acids also results in partial or complete loss of activity.[115,122−124] When either Fe or an α-keto acid is absent, no activity occurs.

The requirement for ascorbate in the catalytic cycle is not as strict since some activity can be detected in its absence. Yet studies with prolyl hydroxylase show that the addition of ascorbate is necessary to obtain full enzymatic activity.[124−126] This requirement is unusual considering that the catalytic reactions do not need an external reducing agent for turnover. In fact, when prolyl hydroxylase is reconstituted with Fe(II) and reacted with α-ketoglutarate and peptidyl proline in the absence of ascorbate, the initial oxidation rate is unaffected, but after 1 min, the enzyme becomes 90% inactivated. This inactivation has been partially attributed to the oxidation of Fe(II) to Fe(III), and addition of ascorbate after the reaction does recover 35% of activity.[127] During normal turnover the enzymatic reaction consumes substoichiometric amouts of ascorbate, but in the

absence of substrate, a stoichiometric amount of ascorbate is consumed, indicating that ascorbate can be oxidized by the enzyme.[124−126] Therefore, these results suggest that ascorbate may serve two purposes, to reduce the inactive Fe(III) form to the active Fe(II) state and to protect the enzymes from oxidative self-inactivation.

Despite the large number of α-keto acid-dependent enzymes, very little is actually known about the coordination environment around the iron center. Unlike the other enzymes discussed in this review, no crystal structure has been reported for any α-keto acid-dependent enzyme. Sequence comparisons of a number of α-keto acid-dependent dioxygenases have demonstrated the presence of several homologous regions, including two regions which contain two His and an Asp residue that are conserved in all the enzymes. Furthermore these conserved His and Asp residues correspond to the His and Asp ligands found for IPNS.[14,98,99,128]

Site-directed mutagenesis and chemical modification experiments support the involvement of histidine residues in the active site. Friedman et al. have shown that a point mutation of His675, one of the conserved His residues, to an alanine in aspartyl β-hydroxylase results in the loss of enzymatic activity.[129] Similarly, Kivirikko et al. have reported that the conversion of three (His412, His483, or His501) of the five conserved His residues found among prolyl 4-hydroxylases to Ser residues completely inactivates the enzyme without disrupting the tertiary structure of the protein.[130] Chemical modification of prolyl 4-hydroxylase[131] and 2,4-dichlorophenoxyacetate dioxygenase[122] with diethyl pyrocarbonate (DEP), a chemical commonly considered a histidine-selective reagent, also causes complete loss of activity in these enzymes. These studies suggest that His residues may act as iron ligands, an assignment consistent with the other mononuclear non-heme iron enzymes discussed in this review.

Very little spectroscopic data has been reported for this class of enzymes. An early EPR study of the as-isolated prolyl hydroxylase showed a weak EPR signal at $g = 4.3$, which is typical of a high-spin Fe(III) center and for which the intensity was modulated by the addition of cofactor and/or ascorbate.[132] However the weakness of this signal suggests that it is a minor species. More recently, *p*-hydroxyphenylpyruvate (HPP) dioxygenase has been found to exhibit an intense EPR signal at $g = 4.3$, indicating all the iron present in the enzyme is in the high-spin Fe(III) state. This enzyme is deep blue (λ_{max} 595 nm) and exhibits a resonance Raman spectrum with features at 583, 1170, 1284, 1503, and 1601 cm^{-1}, characteristic of tyrosinate vibrations.[118] On the basis of these spectroscopic observations, the blue color is assigned to a tyrosinate-to-Fe(III) charge transfer transition. The assignment of a Tyr residue as a ligand is consistent with the sequence comparison of seven HPP dioxygenases from various mammalian and pseudomonad sources, which indicates that a Tyr residue is conserved.[133,134] It is important to note that this blue enzyme species is inactive, but addition of a reductant bleaches the blue color and activates the enzyme.

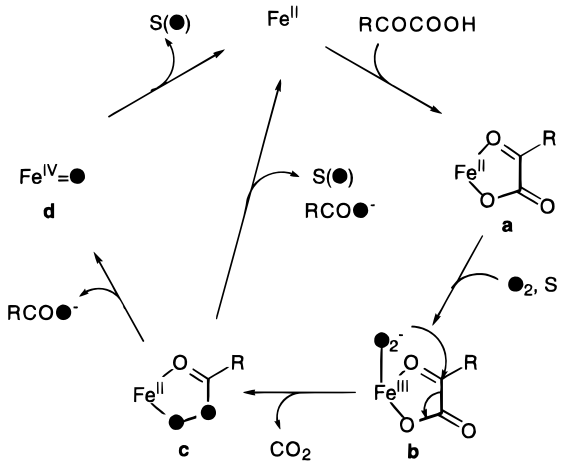

Figure 24. Proposed reaction mechanism of α-keto acid-dependent oxygenases.

Although information about the coordination environment in the active site is limited, a mechanism for the α-keto acid-dependent enzymes has been proposed which is consistent with available kinetic and reactivity studies (Figure 24).[19,115] The initial step of the reaction is proposed to be the ligation of the α-keto acid to Fe(II) (Figure 24a), followed by the addition of O_2, consistent with kinetic studies on prolyl 4-hydroxylase[5,135] and thymine hydroxylase.[136] The binding of the α-keto acid has also been suggested by the DEP experiments, where chemical modification of the proposed His ligands in 2,4-dichlorophenoxyacetate dioxygenase is inhibited by the addition of Fe(II) and α-ketoglutarate, whereas Fe(II) or α-ketoglutarate alone did not prevent the inactivation.[122] After the α-keto acid is bound, O_2 is proposed to bind to the Fe(II) center, forming an Fe(III)−superoxide adduct (Figure 24b), which is consistent with the observation that superoxide scavengers are competitive inhibitors of O_2 consumption.[121,137] Attack of the bound O_2 on the ligated α-keto acid at the C-2 position results in decarboxylation of the α-keto acid to give a Fe(II)−peroxy derivative (Figure 24c) which can react with substrate either directly or via a high-valent iron−oxo intermediate (Figure 24d) to give the oxygenated substrate, a carboxyl acid, and the starting Fe(II) enzyme.

To date none of the species in the proposed mechanism has been characterized spectroscopically in these enzymes; however, recent model studies strongly support this mechanism. Chiou and Que have obtained the first crystal structures of Fe(II) complexed to an α-keto acid, using benzoylformate (BF) as the model α-keto acid.[19,138,139] The α-keto acid moiety can coordinate to the iron either as a monodentate or bidentate ligand (Figure 25). UV/vis spectra for the bidentate-bound Fe^{II}(6-Me_3-TPA)−BF complex has absorbances at 544 nm (ϵ = 690 M^{-1} cm^{-1}) and at 590 nm (ϵ = 600 $M^{-1}cm^{-1}$) which are attributed to Fe(II)-to-BF charge transfer transitions that are absent in the monodentate BF complex. Similar features are observed for the BF complex of Fe^{II}-($Tp^{3,5-Me_2}$).[20]

Exposure of $[Fe^{II}(L)(BF)]^+$ complexes (L = TPA, 6-Me_3-TPA, $Tp^{3,5-Me_2}$) to O_2 results in the quantitative conversion of BF to benzoic acid and CO_2, modeling the oxidative decarboxylation reaction characteristic

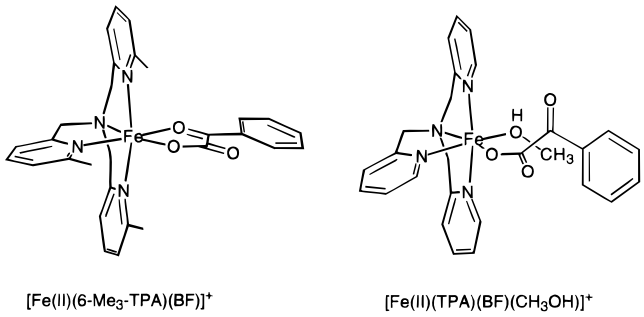

Figure 25. Models for α-keto acid dependent enzymes.

of this class of enzymes.[19,20,139] As with the enzymes, the use of $^{18}O_2$ in the model studies results in the incorporation of the label into the benzoate product. For [Fe(6-Me_3-TPA)BF]$^+$, the rate of the oxidative decarboxylation can be modulated by functional groups on the benzene ring of BF. The trend indicates that increasing the electron-withdrawing ability of the functional groups results in an increase in the rate. The Hammett plot gives a good correlation for relative rates vs σ with a slope (ρ) of +1.07. This pattern of reactivity suggests that the oxidative decarboxylation involves a nucleophilic attack, most plausibly by the iron bound O_2^-, on the keto carbon of BF to initiate decarboxylation (as proposed in Figure 24c). In studies of the enzymes, the decarboxylation of the α-keto acid can be uncoupled from the alkane functionalization step, suggesting that the species responsible for alkane functionalization is generated after decarboxylation.[125,140−143] Thus, the use of substrate analogues that are not oxidized by the enzyme resulted only in the oxidative decarboxylation of the cofactor and the channeling of the oxidizing equivalents generated to the oxidation of ascorbate.

The nature of the active oxidant in these enzymes has not been established; either an iron−peroxy intermediate or a high-valent Fe(IV)−oxo species has been proposed. It has been observed that persuccinic acid, the peroxy acid proposed to be formed after decarboxylation of α-ketoglutarate, cannot substitute for α-ketoglutarate and O_2 in carrying out the prolyl hydroxylase reaction and does not inhibit the binding of the α-keto acid.[140,144] Similarly, 2-(*p*-hydroxyphenyl)peracetic acid does not react with HPP dioxygenase to afford the product of the enzyme reaction.[145] These two observations disfavor an iron−peroxy acid intermediate as the active species. Evidence for an iron−oxo species has been found in studies of thymine hydroxylase and HPP dioxygenase with substrate analogues. Besides the hydroxylation of the 5-methyl group of thymine, thymine hydroxylase can also catalyze allylic hydroxylations, epoxidation of olefins, oxidation of sulfides to sulfoxides, and N-demethylation of amines.[146] HPP dioxygenase has also been shown to catalyze sulfoxidations.[147] This reactivity is similar to that of cytochrome P450 and suggests a similar active intermediate, i.e. a high-valent iron−oxo species. Furthermore, it has been shown in DAOC/DAC synthase[148,149] and HPP dioxygenase[150] that ^{18}O from $H_2{}^{18}O$ can be incorporated into the oxygenated product, which is consistent with an iron−oxo or iron−hydroxyl species in the mechanisms of DAOC/DAC synthase and HPP dioxygenase.

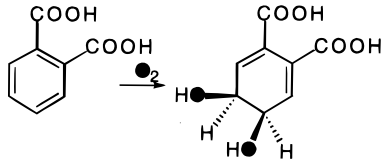

Figure 26. Reaction catalyzed by phthalate dioxygenase.

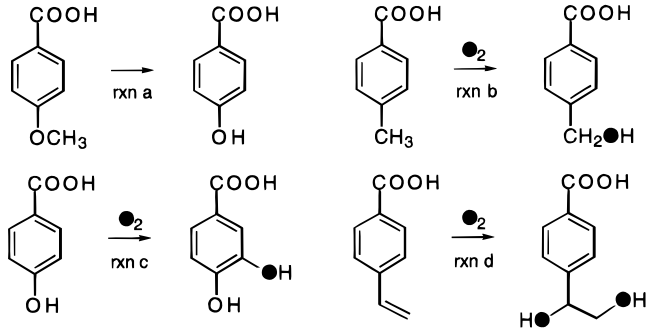

Figure 27. Reactions catalyzed by putidamonoxin.

Further support for an iron-bound active oxidant comes from the study of the $Fe^{II}(Tp^{3,5-Me_2})$(BF) complex.[20] This complex reacts with O_2 to form a species capable of stereospecifically epoxidizing olefins. For example, epoxidation of *cis*-stilbene gives only *cis*-stilbene oxide as the product, but *trans*-stilbene cannot be epoxidized, which suggests that epoxidation occurs at a sterically congested transition state, i.e. near the iron center. More studies are needed to provide insight into the nature of the active oxidant.

VI. Rieske Oxygenases: Non-Heme Iron Analogues of Cytochrome P450

The Rieske oxygenases are involved in the oxygenation of aromatic compounds in the soil.[151] The best studied examples of the Rieske oxygenases are phthalate dioxygenase (PDO)[152,153] and 4-methoxybenzoate O-demethylase (putidamonoxin, PMO).[154−156] PDO catalyzes the *cis*-dihydroxylation of the phthalate C4−C5 double bond (Figure 26) and is representative of other *cis*-dihydroxylating enzymes (e.g. benzoate 1,2-dioxygenase, toluene 2,3-dioxygenase) that catalyze the initial step in the degradation of aromatic rings; the dihydrodiol products serve as precursors to catechols that are cleaved by the catechol dioxygenases discussed earlier. PMO, on the other hand, can function as an O-demethylase and hydroxylate aliphatic and aromatic substrates and convert an alkene into a diol (reactions a−d, respectively, in Figure 27).[157]

The Rieske oxygenases require a mononuclear nonheme iron center and a Rieske-type Fe_2S_2 cluster. Mössbauer studies of PMO show the mononuclear iron to be in the high-spin iron(II) state in the as-isolated enzyme. CD, MCD, and EXAFS studies on PDO indicate that the Fe(II) center has a six-coordinate ligand environment in the as-isolated form that becomes five-coordinate upon substrate binding,[153,158,159] presumably priming it for binding O_2. Indeed, NO binds to PMO to form an $S = 3/2$ (Fe(II)−NO) center;[160] while the NO complex of the as-isolated enzyme exhibits an EPR spectrum indicative of heterogeneity, only one spectral component is observed when the physiological substrate is bound.

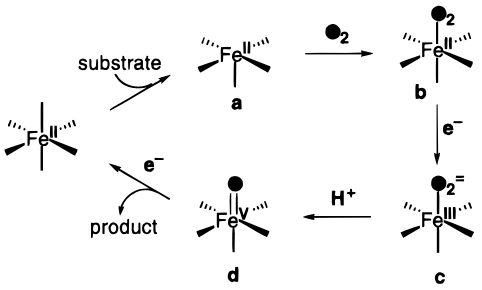

Figure 28. Postulated reaction mechanism for the Rieske oxygenases following the cytochrome P450 paradigm.

The Fe_2S_2 cluster functions to channel electrons from NADH via a reductase to the mononuclear iron center. The Rieske-type Fe_2S_2 center differs from ferredoxin Fe_2S_2 clusters in exhibiting a higher potential (by 100−250 mV) and a more anisotropic EPR spectrum with *g*-values of ca. 1.7, 1.9, and 2.0. EXAFS[161] and ENDOR[162] studies indicate that two histidines have replaced two cysteines while resonance Raman studies show that both histidines are on one iron center; the substitution of two Cys with two His ligands on iron very likely gives rise to the distinct properties of the Rieske cluster.[163]

The mononuclear non-heme iron center and the Rieske cluster thus function respectively like the heme center in cytochrome P450 and its associated iron−sulfur protein (e.g. putidaredoxin in the case of cytoochrome $P450_{cam}$). Since the Rieske oxygenases also carry out reactions that resemble cytochrome P450, the postulated reaction mechanism as illustrated in Figure 28 follows the cytochrome P450 paradigm.[110] The mechanism consists of substrate binding to form a high-spin iron(II) center (Figure 28a), dioxygen binding (Figure 28b), reduction of the oxy complex by one electron to form a peroxoiron(III) intermediate (Figure 28c), O−O bond heterolysis to form a high-valent iron−oxo species (Figure 28d), oxidation of the substrate and reduction of the iron center to the iron(III) state, and transfer of a second electron to reduce the iron back to the iron(II) state.

PMO can functionalize aliphatic and aromatic C−H bonds (Figure 27a−c). The O-demethylation reaction is essentially a hydroxylation of the methoxy group followed by hydrolysis of the hemiformal. However, PMO can also act as a dioxygenase (Figure 27d). The dioxygenation reactions catalyzed by PMO and PDO may distinguish these enzymes from cytochrome P450; indeed an $[FeO_2]^+$ species related to that shown in Figure 28c has been proposed to act as the dioxygenating species.[157,164] However, the conversion of a vinyl side chain to a glycol in Figure 27d can be construed as an epoxidation of the double bond followed by ring opening by the hydroxide derived from O_2 reduction which is trapped in the active site. The stereochemistry of the dihydroxylation product needs to be probed to establish the mechanism of dioxygenation. While these product studies point to reaction intermediates similar to those depicted in the proposed scheme in Figure 28, none of the three key oxygenated intermediates (oxy adduct, peroxo intermediate, and high-valent iron−oxo species) has to date been observed for the Rieske oxygenases.

Evidence to support such intermediates has been found in the chemistry of bleomycin, a natural product that requires Fe(II) for its antitumor activity.[165−167] Fe(II)−bleomycin catalyzes the oxidation of a number of substrates via a mechanism that is analogous to that shown in Figure 28 and may serve as a model for the mononuclear non-heme iron center in the Rieske oxygenases. As with the Rieske oxygenases, Fe^{II}BLM is a mononuclear non-heme iron complex that requires O_2 and an external reducing agent in its catalytic cycle. On the basis of a number of spectroscopic studies, particularly recent 2D NMR results on the diamagnetic hydroperoxocobalt(III) derivative[168] and the paramagnetic iron(II) complex,[169] as well as on model studies by the Mascharak group,[21] BLM is proposed to coordinate to the Fe center via five ligands, as shown in Figure 29. The sixth coordination site is therefore available to bind O_2.

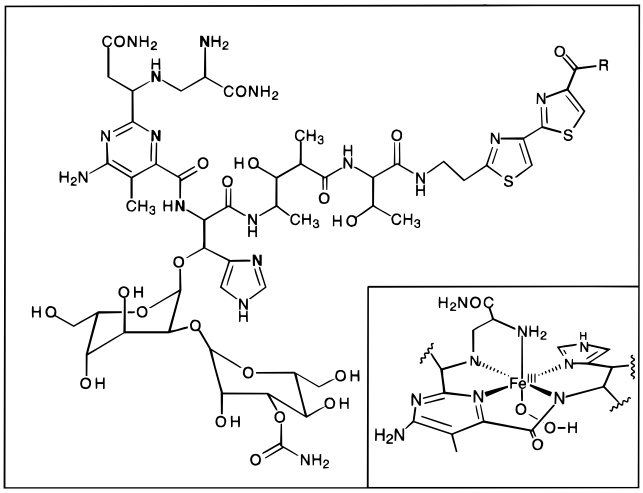

Figure 29. Bleomycin and the iron coordination in bleomycin. (The bold atoms represent the iron-binding ligands.)

Spectroscopic studies following the reaction of Fe^{II}BLM and O_2 have identified two transient species. Upon exposure to O_2, the EPR-silent, high-spin Fe^{II}BLM[170,171] is rapidly converted to $Fe^{II}BLM-O_2$, the Mössbauer parameters of which are most consistent with an Fe(III)−superoxide species.[172] The introduction of an electron converts the oxy form to "activated bleomycin" which corresponds to the last detectable intermediate prior to the oxidation of substrate. This intermediate, which can also be obtained by the reaction of Fe(III)BLM and H_2O_2, has been characterized by electrospray mass spectrometry to be a (BLM)Fe−OOH complex.[173] The iron center is deduced to be in the low-spin iron(III) state on the basis of EPR, Mössbauer, and XAS evidence.[170,172,174,175]

A significant point of discussion is whether the hydroperoxoiron(III) intermediate is directly responsible for the oxidation chemistry or whether it does so via a high-valent iron−oxo species, by analogy to cytochrome P450. An important argument has been that, like cytochrome P450, Fe(III)BLM and PhIO can carry out the oxidation of organic substrates.[176,177] However, the demonstration that PhIO can be activated by interaction with redox-inactive Lewis acids to effect the observed oxidations has blunted this argument somewhat.[178,179] Furthermore there is increasing skepticism as to whether a formally iron(V) species can be obtained without a porphyrin ligand to aid in delocalizing the oxidizing equivalents,

as has been established for heme peroxidase compound **I**. The issue of whether peroxometal species can be responsible for some biological reactions has been raised in a number of contexts, including methane monooxygenase,[180] dopamine β-hydroxylase,[181] and even cytochrome P450.[182−184] Recently the first established synthetic examples of low-spin iron(III) hydroperoxide and alkylperoxide complexes analogous to "activated bleomycin" have been characterized.[185−187] It has been shown in one case that the cleavage of the peroxo O−O bond is concomitant with the cleavage of the substrate C−H bond, providing the first evidence that a peroxoiron species can directly oxidize aliphatic C−H bonds.[187] These studies demonstrate that many mechanisic questions remain to be answered in elucidating the role of mononuclear non-heme iron centers in oxygen activation.

VII. Perspectives

We have reviewed the available information to date regarding the structures and mechanisms of a number of mononuclear non-heme iron enzymes that activate dioxygen. The dramatic increase in structural information on these enzymes in the past few years derived from site-directed mutagenesis, spectroscopy, and, in particular, X-ray crystallography has set the stage for a systematic comparison of enzyme active sites and their roles in catalysis. In general, the enzymes that are active in the Fe(III) state take advantage of the Lewis acidity of the iron center to activate substrates to react with O_2; the iron center becomes involved in dioxygen binding only after O_2 has been reduced to the peroxide level. The Fe(II) enzymes, on the other hand, are likely to bind O_2 directly, often after substrate or cofactor binding has primed the Fe(II) center. The various mechanisms discussed here appear to have a common thread with only the details differing from enzyme to enzyme. As our efforts to understand these enzymes develop and mature, it will be interesting to discover how the various active sites control the metal environment and tailor the iron chemistry to effect the myriad transformations these enzymes catalyze.

VIII. Abbreviations

ACV	δ-(L-α-aminoadipoyl)-L-cysteinyl-D-valine
BF	benzoylformate
BLM	bleomycin
BphC	2,3-dihydroxybiphenyl 1,2-dioxygenase
BPMP-H	2,6-bis[bis(2-pyridylmethyl)aminomethyl]-4-methylphenol
CD	circular dichroism
CTD	catechol dioxygenase
DAC	deacetylcephalosporin C
DAOC	deacetoxycephalosporin C
$DBCH_2$	3,5-di-*tert*-butylcatechol
DEP	diethyl pyrocarbonate
DOPA	3,4-dihydroxyphenylalanine
ESEEM	electon spin-echo envelope modulation
EPR	electron paramagnetic resonance
EXAFS	extended X-ray absorption fine structure
HPP	*p*-hydroxyphenylpyruvate
IPNS	isopenicillin N synthase
α-KG	α-ketoglutarate
MCD	magnetic circular dichroism
$6\text{-}Me_3\text{-}TPA$	tris[(6-methyl-2-pyridyl)methyl]amine
MndD	3,4-dihydroxyphenylacetate 2,3-dioxygenase
NMR	nuclear magnetic resonance
NTA	nitrilotriacetate
OAc	acetate
OBz	benzoate
PCD	protocatechuate dioxygenase
PDO	phthalate dioxygenase
PMA-H	2-(2′,5′-diazapentyl)-5-bromopyrimidine-6-carboxylic acid *N*-[2-(4′-imidazolyl)ethyl]amide
PMO	putidamonoxin (4-methoxybenzoate O-demethylase)
SLO-1	soybean lipoxygenase-1
TACN	triazacyclononane
TPA	tris(2-pyridylmethyl)amine
$Tp^{3,5\text{-}Me_2}$	hydrotris(3,5-dimethyl pyrazolyl)borate
XANES	X-ray absorption near-edge spectroscopy
XAS	X-ray absorption spectroscopy

IX. Acknowledgments

L.Q.'s research program on mononuclear non-heme iron oxygen-activating enzymes has been generously supported by the National Institutes of Health (GM-33162). R.Y.N.H. acknowledges a National Institutes of Health postdoctoral fellowship (GM-17849). The authors would like to thank Allen M. Orville, Prof. Douglas H. Ohlendorf, and Prof. John D. Lipscomb for providing Figure 4.

X. References

(1) *Microbial Degradation of Organic Molecules*; Gibson, D. T., Ed.; Marcel Dekker: New York, 1984, pp 535.
(2) Nelson, M. J.; Seitz, S. In *Active Oxygen in Biochemistry*; Valentine, J. S., Foote, C. S., Greenberg, A., Liebman, J. F., Eds.; Chapman and Hall: Glasgow, U.K., 1995; pp 276−312.
(3) Baldwin, J. E.; Bradley, M. *Chem. Rev.* **1990**, *90*, 1079−1088.
(4) Baldwin, J. E.; Adlington, R. M.; Crouch, N. P.; Schofield, C. J.; Turner, N. J.; Aplin, R. T. *Tetrahedron* **1991**, *47*, 9881−9900.
(5) Kivirikko, K. I.; Myllylä, R.; PihlaJaniemi, T. *FASEB J.* **1989**, *3*, 1609−1617.
(6) Stenflo, J.; Holme, E.; Lindstedt, S.; Chandramouli, N.; Tsai Huang, L. H.; Tam, J. P.; Merrifield, R. B. *Proc. Natl. Acad. Sci. U.S.A.* **1989**, *86*, 444−447.
(7) Feig, A. L.; Lippard, S. J. *Chem. Rev.* **1994**, *94*, 759−805.
(8) Ohlendorf, D. H.; Lipscomb, J. D.; Weber, P. C. *Nature (London)* **1988**, *336*, 403−405.
(9) Ohlendorf, D. H.; Orville, A. M.; Lipscomb, J. D. *J. Mol. Biol.* **1994**, *244*, 586−608.
(10) Han, S.; Eltis, L. D.; Timmis, K. N.; Muchmore, S. W.; Bolin, J. T. *Science* **1995**, *270*, 976−980.
(11) Senda, T.; Sugiyama, K.; Narita, H.; Yamamoto, T.; Kimbara, K.; Fukuda, M.; Sato, M.; Yano, K.; Mitsui, Y. *J. Mol. Biol.* **1996**, *255*, 735−752.
(12) Boyington, J. C.; Gaffney, B. J.; Arnzel, M. *Science* **1993**, *260*, 1482−1486.
(13) Minor, W.; Steczko, J.; Bolin, J. T.; Otwinowski, Z.; Axelrod, B. *Biochemistry* **1993**, *32*, 6320−6323.
(14) Roach, P. L.; Clifton, I. J.; Fülöp, V.; Harlos, K.; Barton, G. J.; Hajdu, J.; Andersson, I.; Schofield, C. J.; Baldwin, J. E. *Nature* **1995**, *375*, 700−704.
(15) Jang, H. G.; Cox, D. D.; Que, L., Jr. *J. Am. Chem. Soc.* **1991**, *113*, 9200−9204.
(16) Dei, A.; Gatteschi, D.; Pardi, L. *Inorg. Chem.* **1993**, *32*, 1389−1395.
(17) Zang, Y.; Elgren, T. E.; Dong, Y.; Que, L., Jr. *J. Am. Chem. Soc.* **1993**, *115*, 811−813.
(18) Zang, Y.; Que, L., Jr. *Inorg. Chem.* **1995**, *34*, 1030−1035.
(19) Chiou, Y.-M.; Que, L., Jr. *J. Am. Chem. Soc.* **1995**, *117*, 3999−4013.
(20) Ha, E. H.; Ho, R. Y. N.; Kisiel, J. F.; Valentine, J. S. *Inorg. Chem.* **1995**, *34*, 2265−2266.
(21) Guajardo, R. J.; Hudson, S. E.; Brown, S. J.; Mascharak, P. K. *J. Am. Chem. Soc.* **1993**, *115*, 7971−7977.
(22) Lipscomb, J. D.; Orville, A. M. *Metal Ions Biol. Syst.* **1992**, *28*, 243−298.
(23) Que, L., Jr. In *Iron Carriers and Iron Proteins*; Loehr, T. M., Ed.; VCH: New York, 1989; pp 467−524.

(24) Que, L., Jr.; Widom, J.; Crawford, R. L. *J. Biol. Chem.* **1981**, *256*, 10941−10944.
(25) Boldt, Y. R.; Sadowsky, M. J.; Ellis, L. B. M.; Que, L., Jr.; Wackett, L. P. *J. Bacteriol.* **1995**, *177*, 1225−1232.
(26) Whiting, A. K.; Boldt, Y. R.; Hendrich, M. P.; Wackett, L. P.; Que, L., Jr. *Biochemistry* **1996**, *35*, 160−170.
(27) Pyrz, J. W.; Roe, A. L.; Stern, L. J.; Que, L., Jr. *J. Am. Chem. Soc.* **1985**, *107*, 614−620.
(28) Que, L., Jr.; Heistand, R. H., II; Mayer, R.; Roe, A. L. *Biochemistry* **1980**, *19*, 2288−2293.
(29) Que, L., Jr.; Epstein, R. M. *Biochemistry* **1981**, *20*, 2545−2549.
(30) Siu, C.-T.; Orville, A. M.; Lipscomb, J. D.; Ohlendorf, D. H.; Que, L., Jr. *Biochemistry* **1992**, *31*, 10443−10448.
(31) Felton, R. H.; Barrow, W. L.; May, S. W.; Sowell, A. L.; Goel, S.; Bunker, G.; Stern, E. A. *J. Am. Chem. Soc.* **1982**, *22*, 6132−6134.
(32) Whittaker, J. W.; Lipscomb, J. D. *J. Biol. Chem.* **1984**, *259*, 4487−4495.
(33) True, A. E.; Orville, A. M.; Pearce, L. L.; Lipscomb, J. D.; Que, L., Jr. *Biochemistry* **1990**, *29*, 10847−10854.
(34) Whittaker, J. W.; Lipscomb, J. D.; Kent, T. A.; Münck, E. *J. Biol. Chem.* **1984**, *259*, 4466−4475.
(35) Que, L., Jr.; Lipscomb, J. D.; Zimmermann, R.; Münck, E.; Orme-Johnson, N. R.; Orme-Johnson, W. H. *Biochim. Biophys. Acta* **1976**, *452*, 320−334.
(36) Que, L., Jr.; Heistand, R. H., II. *J. Am. Chem. Soc.* **1979**, *101*, 2219−2221.
(37) Felton, R. H.; Cheung, L. D.; Phillips, R. S.; May, S. W. *Biochem. Biophys. Res. Commun.* **1978**, *85*, 844−850.
(38) Orville, A. M.; Lipscomb, J. D. *J. Biol. Chem.* **1989**, *264*, 8791−8801.
(39) Lauffer, R. B.; Que, L., Jr. *J. Am. Chem. Soc.* **1982**, *104*, 7324−7325.
(40) Elgren, T. E.; Que, L., Jr., unpublished observations.
(41) Orville, A. M.; Ohlendorf, D. H.; Lipscomb, J. D. unpublished results.
(42) Nozaki, M. In *Molecular Mechanisms of Oxygen Activation*; Hayaishi, O., Ed.; Academic Press: New York, 1974; pp 135−165.
(43) Orville, A. M.; Lipscomb, J. D. *J. Biol. Chem.* **1993**, *268*, 8596−8607.
(44) Walsh, T. A.; Ballou, D. P.; Mayer, R.; Que, L., Jr. *J. Biol. Chem.* **1983**, *258*, 14422−14427.
(45) Bull, C.; Ballou, D. P.; Otsuka, S. *J. Biol. Chem.* **1981**, *256*, 12681−12686.
(46) Que, L., Jr.; Lipscomb, J. D.; Münck, E.; Wood, J. M. *Biochim. Biophys. Acta* **1977**, *485*, 60−74.
(47) Que, L., Jr.; Kolanczyk, R. C.; White, L. S. *J. Am. Chem. Soc.* **1987**, *109*, 5373−5380.
(48) Cox, D. D.; Que, L., Jr. *J. Am. Chem. Soc.* **1988**, *110*, 8085−8092.
(49) Bianchini, C.; Frediani, P.; Laschi, F.; Meli, A.; Vizza, F.; Zanello, P. *Inorg. Chem.* **1990**, *29*, 3402−3409.
(50) Barbaro, P.; Bianchini, C.; Linn, K.; Mealli, C.; Meli, A.; Vizza, F.; Laschi, F.; Zanello, P. *Inorg. Chim. Acta* **1992**, *198*−200, 31−56.
(51) Barbaro, P.; Bianchini, C.; Mealli, C.; Meli, A. *J. Am. Chem. Soc.* **1991**, *113*, 3181−3183.
(52) Koch, W. O.; Krüger, H.-J. *Angew. Chem. Int. Ed. Engl.* **1995**, *34*, 2671−2674.
(53) Mayer, R. J.; Que, L., Jr. *J. Biol. Chem.* **1984**, *259*, 13056−13060.
(54) Mabrouk, P. A.; Orville, A. M.; Lipscomb, J. D.; Solomon, E. I. *J. Am. Chem. Soc.* **1991**, *113*, 4053−4061.
(55) Shu, L.; Chiou, Y.-M.; Orville, A. M.; Miller, M. A.; Lipscomb, J. D.; Que, L., Jr. *Biochemistry* **1995**, *34*, 6649−6659.
(56) Bertini, I.; Briganti, F.; Mangani, S.; Nolting, H. F.; Scozzafava, A. *Biochemistry* **1994**, *33*, 10777−10784.
(57) Bertini, I.; Capozzi, F.; Dikiy, A.; Happe, B.; Luchinat, C.; Timmis, K. N. *Biochem. Biophys. Res. Commun.* **1995**, *215*, 855−860.
(58) Arciero, D. M.; Orville, A. M.; Lipscomb, J. D. *J. Biol. Chem.* **1985**, *260*, 14035−14044.
(59) Bolin, J. T., personal communication.
(60) Arciero, D. M.; Lipscomb, J. D. *J. Biol. Chem.* **1986**, *261*, 2170−2178.
(61) Chiou, Y. M.; Que, L., Jr. *Inorg. Chem.* **1995**, *34*, 3577−3578.
(62) Ballou, D. P.; C., B. In *Biochemical and Clinical Aspects of Oxygen.*; Caughey, W., Ed.; Academic Press: New York, 1980; pp 573−587.
(63) Ito, M.; Que, L., Jr. Unpublished results.
(64) Sanvoisin, J.; Langley, G. J.; Bugg, T. D. H. *J. Am. Chem. Soc.* **1995**, *117*, 7836−7837.
(65) Harpel, M. R.; Lipscomb, J. D. *J. Biol. Chem.* **1990**, *265*, 22187−22196.
(66) Siedow, J. N. *Annu. Rev. Plant Physiol. Mol. Biol.* **1991**, *42*, 145−188.
(67) Gardner, H. W. *Biochim. Biophys. Acta* **1991**, *1084*, 221−239.
(68) Ford-Hutchinson, A. W.; Gresser, M.; Young, R. N. *Annu. Rev. Biochem.* **1994**, *63*, 383−417.
(69) Steczko, J.; Axelrod, B. *Biochem. Biophys. Res. Commun.* **1992**, *186*, 686−689.
(70) Steczko, J.; Donoho, G. P.; Clemens, J. C.; Dixon, J. E.; Axelrod, B. *Biochemistry* **1992**, *31*, 4053−4057.
(71) Cox, D. D.; Benkovic, S. J.; Bloom, L. M.; Bradley, F. C.; Nelson, M. J.; Que, L., Jr.; Wallick, D. E. *J. Am. Chem. Soc.* **1988**, *110*, 2026−2032.
(72) Kramer, J. A.; Johnson, K. R.; Dunham, K. R.; Sands, R. H.; Funk, M. O., Jr. *Biochemistry* **1994**, *33*, 15017−15022.
(73) Solomon, E. I.; Pavel, E. G.; Loeb, K. E.; Campochiaro, C. *Coord. Chem. Rev.* **1995**, *144*, 369−460.
(74) Nelson, M. J. *J. Biol. Chem.* **1987**, *262*, 12137−12142.
(75) Feiters, M. C.; Aasa, R.; Malmström, B. G.; Veldink, G. A.; Vliegenthart, J. F. G. *Biochim. Biophys. Acta* **1986**, *873*, 182−189.
(76) Scarrow, R. C.; Trimitsis, M. G.; Buck, C. P.; Grove, G. N.; Cowling, R. A.; Nelson, M. J. *Biochemistry* **1994**, *33*, 15023−15035.
(77) Van der Heijdt, L. M.; Feiters, M. C.; Navaratnam, S.; Nolting, H.-F.; Hermes, C.; Veldink, G.; Vliegenthart, J. F. G. *Eur. J. Biochem.* **1992**, *207*, 793−802.
(78) Zhang, Y.; Gebhard, M. S.; Solomon, E. I. *J. Am. Chem. Soc.* **1991**, *113*, 5162−5175.
(79) Nelson, M. J. *J. Am. Chem. Soc.* **1988**, *110*, 2985−2986.
(80) de Groot, J. J. M. C.; Garssen, G. J.; Veldink, G. A.; Vliegenthart, J. F. G.; Boldingh, J. *FEBS Lett.* **1975**, *56*, 50−54.
(81) Chasteen, N. D.; Grady, J. K.; Skorey, K. I.; Neden, K. J.; Riendeau, D.; Percival, M. D. *Biochemistry* **1993**, *32*, 9763−9771.
(82) Zhang, Y.; Gan, Q.-F.; Pavel, E. G.; Sigal, E.; Solomon, E. I. *J. Am. Chem. Soc.* **1995**, *117*, 7422−7427.
(83) Egmond, M. R.; Fasella, P. M.; Veldink, G. A.; Vliegenthart, J. F. G.; Boldingh, J. *Eur. J. Biochem.* **1977**, *76*, 469−479.
(84) de Groot, J. J. M. C.; Garssen, G. J.; Vliegenthart, J. F. G.; Boldingh, J. *Biochim. Biophys. Acta* **1973**, *326*, 279−284.
(85) Corey, E. J.; Nagata, R. *J. Am. Chem. Soc.* **1987**, *109*, 8107−8108.
(86) Nelson, M. J.; Cowling, R. A. *J. Am. Chem. Soc.* **1990**, *112*, 2820−2821.
(87) Nelson, M. J.; Seitz, S. P.; Cowling, R. A. *Biochemistry* **1990**, *29*, 6897−6903.
(88) Hwang, C. C.; Grissom, C. B. *J. Am. Chem. Soc.* **1994**, *116*, 795−796.
(89) Glickman, M. H.; Wiseman, J. S.; Klinman, J. P. *J. Am. Chem. Soc.* **1994**, *116*, 793−794.
(90) Glickman, M. H.; Klinman, F. P. *Biochemistry* **1995**, *34*, 14077−14092.
(91) Bill, T. J.; Chen, S.; Pascal, R. A.; Schwartz, J. *J. Am. Chem. Soc.* **1990**, *112*, 9019−9020.
(92) Nelson, M. J. *Biochemistry* **1988**, *27*, 4273−4278.
(93) *Encyclopedia of Electrochemistry of Elements*; Bard, A. J., Ed.; Marcel Dekker: New York, 1978; Vol. XI.
(94) Gardner, K. A.; Mayer, J. M. *Science* **1995**, *269*, 1849−1851.
(95) Cook, G. K.; Mayer, J. M. *J. Am. Chem. Soc.* **1995**, *117*, 7139−7156.
(96) McMillen, D. F.; Golden, D. M. *Ann. Rev. Phys. Chem.* **1982**, *33*, 493−532.
(97) Zang, Y.; Pan, G.; Que, L., Jr.; Fox, B. G.; Münck, E. *J. Am. Chem. Soc.* **1994**, *116*, 3653−3654.
(98) Borovok, H.; Landman, O.; Kriesberg, R.; Aharonowitz, Y.; Cohen, G. *Biochem* **1996**, *35*, 1981−1987.
(99) Tan, D. S. H.; Sim, T.-S. *J. Biol. Chem.* **1996**, *271*, 889−894.
(100) Jiang, J.; Peisach, J.; Ming, L.-J.; Que, L., Jr.; Chen, V. J. *Biochemistry* **1991**, *30*, 11437−11445.
(101) Ming, L.-J.; Que, L., Jr.; Kriauciunas, A.; Frolik, C. A.; Chen, V. J. *Biochemistry* **1991**, *30*, 11653−11659.
(102) Chen, V. J.; Orville, A. M.; Harpel, M. R.; Frolik, C. A.; Surerus, K. K.; Münck, E.; Lipscomb, J. D. *J. Biol. Chem.* **1989**, *264*, 21677−21681.
(103) Ming, L.-J.; Que, L., Jr.; Kriauciunas, A.; Frolik, C. A.; Chen, V. J. *Inorg. Chem.* **1990**, *29*, 1111−1112.
(104) Randall, C. R.; Zang, Y.; True, A. E.; Que, L., Jr.; Charnock, J. M.; Garner, C. D.; Fujishima, Y.; Schofield, C. J.; Baldwin, J. E. *Biochemistry* **1993**, *32*, 6664−6673.
(105) Scott, R. A.; Wang, S.; Eidsness, M. K.; Kriauciunas, A.; Frolik, C. A.; Chen, V. J. *Biochemistry* **1992**, *31*, 4596−4601.
(106) Baldwin, J. E.; Adlington, R. M.; Moroney, S. E.; Field, L. D.; Ting, H.-H. *J. Chem. Soc. Chem. Commun.* **1984**, 984−986.
(107) Baldwin, J. E.; Lynch, G. P.; Schofield, C. J. *Tetrahedron* **1992**, *48*, 9085−9100.
(108) Baldwin, J. E.; Norris, W. J.; Freeman, R. T.; Bradley, M.; Adlington, R. M.; Long-Fox, S.; Schofield, C. J. *J. Chem. Soc., Chem. Commun.* **1988**, 1128−1130.
(109) Baldwin, J. E.; Adlington, R. M.; Bradley, M.; Pitt, A. R.; Turner, N. J. *J. Chem. Soc. Chem. Commun.* **1989**, 978−981.
(110) *Cytochrome P450: Structure, Mechanism, and Biochemistry*; Ortiz de Montellano, P. R., Ed.; Plenum: New York, 1985.
(111) Baldwin, J. E.; Adlington, R. M.; Domayne-Hayman, B. P.; Knight, G.; Ting, H.-H. *J. Chem. Soc., Chem. Commun.* **1987**, 1661−1663.

(112) Kojima, T.; Leising, R. A.; Yan, S.; Que, L., Jr. *J. Am. Chem. Soc.* **1993**, *115*, 11328−11335.
(113) Leising, R. A.; Zang, Y.; Que, L., Jr. *J. Am. Chem. Soc.* **1991**, *113*, 8555−8557.
(114) Abbott, M. T.; Udenfriend, S. In *Molecular Mechanisms of Oxygen Activation*; Hayaishi, O., Ed.; Academic Press: New York, 1974; pp 167−214.
(115) Hanauske-Abel, H. M.; Gunzler, V. *J. Theor. Biol.* **1982**, *94*, 421−455.
(116) Salowe, S. P.; Marsh, E. N.; Townsend, C. A. *Biochemistry* **1990**, *29*, 6499−6508.
(117) Baldwin, J. E.; Abraham, E. *Nat. Prod. Rep.* **1988**, *5*, 129−145.
(118) Bradley, F. C.; Lindstedt, S.; Lipscomb, J. D.; Que, L., Jr.; Roe, A. L.; Rundgren, M. *J. Biol. Chem.* **1986**, *261*, 11693−11696.
(119) Lindstedt, S.; Rundgren, M. *J. Biol. Chem.* **1982**, *257*, 11922−11931.
(120) Rapaka, R. S.; Sorensen, K. R.; Lee, S. D.; Rajendra, S. *Biochim. Biophys. Acta* **1976**, *429*, 63−71.
(121) Tuderman, L.; Myllylä, R.; Kivirikko, K. I. *Eur. J. Biochem.* **1977**, *80*, 341−348.
(122) Fukumori, F.; Hausinger, R. P. *J. Biol. Chem.* **1993**, *268*, 24311−24317.
(123) Ng, S.-F.; Hanauske-Abel, H. M.; Englard, S. *J. Biol. Chem.* **1991**, *266*, 1526−1533.
(124) Majamaa, K.; Hanauske-Abel, H. M.; Gunzler, V.; Kivirikko, K. I. *Eur. J. Biochem.* **1984**, *138*, 239−245.
(125) Myllylä, R.; Majamaa, K.; Gunzler, V.; Hanauske-Abel, H. M.; Kivirikko, K. I. *J. Biol. Chem.* **1984**, *259*, 5403−5405.
(126) Nietfeld, J. J.; Kemp, A. *Biochim. Biophys. Acta* **1981**, *657*, 159−167.
(127) Myllylä, R.; Kuutti-Savolainen, E.-R.; Kivirikko, K. I. *Biochem. Biophys. Res. Commun.* **1978**, *83*, 441−448.
(128) Pirrung, M. C.; Kaiser, L. M.; Chen, J. *Biochemistry* **1993**, *32*, 7445−7450.
(129) Jia, S.; McGinnis, K.; VanDusen, W. J.; Burke, C. J.; Kuo, A.; Griffin, P. R.; Sardana, M. K.; Elliston, K. O.; Stern, A. M.; Friedman, P. A. *Proc. Natl. Acad. Sci. U.S.A.* **1994**, *91*, 7227−7231.
(130) Lamberg, A.; Pihlajaniemi, T.; Kivirikko, K. I. *J. Biol. Chem.* **1995**, *270*, 9926−9931.
(131) Myllylä, R.; Gunzler, V.; Kivirikko, K. I.; Kaska, D. D. *Biochem. J.* **1992**, *286*, 923−927.
(132) De Jong, L.; Albracht, S. P. J.; Kemp, A. *Biochim. Biophys. Acta* **1982**, *704*, 326−331.
(133) Rüetschi, U.; Odelhög, B.; Lindstedt, S.; Barros-Söderling, J.; Persson, B.; Jörnvall, H. *Eur. J. Biochem.* **1992**, *205*, 459−466.
(134) Rüetschi, U.; Déllsen, A.; Sahlin, P.; Stenman, G.; Rymo, L.; Lindstedt, S. *Eur. J. Biochem.* **1993**, *213*, 1081−1089.
(135) Myllylä, R.; Tuderman, L.; Kivirikko, K. I. *Eur. J. Biochem.* **1977**, *80*, 349−357.
(136) Holme, E. *Biochemistry* **1975**, *14*, 4999−5003.
(137) Myllylä, R.; Schubotz, L. M.; Weser, U.; Kivirikko, K. I. *Biochem. Biophys. Res. Commun.* **1979**, *89*, 98−102.
(138) Chiou, Y.-M.; Que, L., Jr. *Angew. Chem. Int. Ed. Engl.* **1994**, *33*, 1886−1888.
(139) Chiou, Y.-M.; Que, L., Jr. *J. Am. Chem. Soc.* **1992**, *114*, 7567−7568.
(140) Counts, D. F.; Cardinale, G. J.; Udenfriend, S. *Proc. Natl. Acad. Sci. U.S.A.* **1978**, *75*, 2145−2149.
(141) Holme, E.; Lindstedt, G.; Lindstedt, S. *Acta Chem. Scand., Ser. B* **1979**, *B33*, 621−622.
(142) Holme, E.; Lindstedt, S.; Nordin, I. *Biochem. Biophys. Res. Commun.* **1982**, *107*, 518−524.
(143) Puistola, U.; Turpeenniemi-Hujanen, T. M.; Myllylä, R.; Kivirikko, K. I. *Biochim. Biophys. Acta* **1980**, *611*, 40−50.
(144) Cardinale, G. J.; Udenfriend, S. *Adv. Enzymol.* **1974**, *41*, 245−300.
(145) Jefford, C. W.; Cadby, A. *Experientia* **1981**, *37*, 1134−1137.
(146) Thornburg, L. D.; Lai, M.-T.; Wishnok, J. S.; Stubbe, J. *Biochemistry* **1993**, *32*, 14023−14033.
(147) Pascal, R. A., Jr.; Oliver, M. A.; Chen, Y.-C. J. *Biochemistry* **1985**, *24*, 3158−3165.
(148) Baldwin, J. E.; Adlington, R. M.; Crouch, N. P.; Pereira, I. A. C. *Tetrahedron* **1993**, *49*, 7499−7518.
(149) Baldwin, J. E.; Adlington, R. M.; Crouch, N. P.; Pereira, I. A. C.; Aplin, R. T.; Robinson, C. *J. Chem. Soc., Chem. Commun.* **1993**, 105−108.
(150) Lindblad, B.; Lindstedt, G.; Lindstedt, S. *J. Am. Chem. Soc.* **1970**, *92*, 7446−7449.
(151) Mason, J. R.; Cammack, R. *Annu. Rev. Microbiol.* **1992**, *46*, 277−305.
(152) Batie, C. J.; LaHaie, E.; Ballou, D. P. *J. Biol. Chem.* **1987**, *262*, 1510−1518.
(153) Gassner, G. T.; Ballou, D. P.; Landrum, G. A.; Whittaker, J. W. *Biochemistry* **1993**, *32*, 4820−4825.
(154) Bernhardt, F.-H.; Kuthan, H. *Eur. J. Biochem.* **1981**, *120*, 547−555.
(155) Bill, E.; Bernhardt, F.-H.; Trautwein, A. X.; Winkler, H. *Eur. J. Biochem.* **1985**, *147*, 177−182.
(156) Twilfer, H.; Bernhardt, F.-H.; Gersonde, K. *Eur. J. Biochem.* **1985**, *147*, 171−176.
(157) Wende, P.; Bernhardt, F.-H.; Pfleger, K. *Eur. J. Biochem.* **1989**, *181*, 189−197.
(158) Tsang, H.-T.; Batie, C. J.; Ballou, D. P.; Penner-Hahn, J. E. *J. Biol. Inorg. Chem.* **1996**, *1*, 24−33.
(159) Pavel, E. G.; Martins, L. J.; Ellis, W. R., Jr.; Solomon, E. I. *Chem., & Biol.* **1994**, *1*, 173−183.
(160) Twilfer, H.; Bernhardt, F.-H.; Gersonde, K. *Eur. J. Biochem.* **1985**, *147*, 171−176.
(161) Tsang, H.-T.; Batie, C. J.; Ballou, D. P.; Penner-Hahn, J. E. *Biochemistry* **1989**, *28*, 7233−7240.
(162) Gurbiel, R. J.; Ohnishi, T.; Robertson, D. E.; Daldal, F.; Hoffman, B. M. *Biochemistry* **1991**, *30*, 11579−11584.
(163) Kuila, D.; Fee, J. A.; Schoonover, J. R.; Woodruff, W. H. *J. Am. Chem. Soc.* **1987**, *109*, 1559−1561.
(164) Ballou, D.; Batie, C. In *Oxidases and Related Redox Systems*; King, T. E., Mason, H. S., Morrison, M., Eds.; Alan R. Liss, Inc.: New York, 1988; pp 211−226.
(165) Stubbe, J.; Kozarich, J. W.; Wu, W.; Vanderwall, D. E. *Acc. Chem. Res.* **1996**, *29*, 322−330.
(166) Stubbe, J.; Kozarich, J. W. *Chem. Rev.* **1987**, *87*, 1107−1136.
(167) Kane, S. A.; Hecht, S. M. *Prog. Nucleic Acid Res. Mol. Biol.* **1994**, 313−352.
(168) Wu, W.; Vanderwall, D. E.; Lui, S. M.; Tang, X. J.; Turner, C. J.; Kozarich, J. W.; Stubbe, J. *J. Am. Chem. Soc.* **1996**, *118*, 1268−1280.
(169) Lehmann, T. E.; Que, L., Jr., submitted.
(170) Burger, R. M.; Peisach, J.; Horwitz, S. B. *J. Biol. Chem.* **1981**, *256*, 11636−11644.
(171) Burger, R. M.; Horwitz, S. B.; Peisach, J.; Wittenberg, J. B. *J. Biol. Chem.* **1979**, *254*, 12299−12302.
(172) Burger, R. M.; Kent, T. A.; Horwitz, S. B.; Münck, E.; Peisach, J. *J. Biol. Chem.* **1983**, *258*, 1559−1564.
(173) Sam, J. W.; Tang, X.-J.; Peisach, J. *J. Am. Chem. Soc.* **1994**, *116*, 5250−5256.
(174) Westre, T. E.; Loeb, K. E.; Zaleski, J. M.; Hedman, B.; Hodgson, K. O.; Solomon, E. I. *J. Am. Chem. Soc.* **1995**, *117*, 1309−1313.
(175) Burger, R. M.; Blanchard, J. S.; Horwitz, S. B.; Peisach, J. *J. Biol. Chem.* **1985**, *260*, 15406−15409.
(176) Murugesan, N.; Hecht, S. M. *J. Am. Chem. Soc.* **1985**, *107*, 493−500.
(177) Heimbrook, D. C.; Carr, S. A.; Mentzer, M. A.; Long, E. C.; Hecht, S. M. *Inorg. Chem.* **1987**, *26*, 3835−3836.
(178) Nam, W.; Valentine, J. S. *J. Am. Chem. Soc.* **1990**, *112*, 4977−4979.
(179) Yang, Y. H.; Diederich, F.; Valentine, J. S. *J. Am. Chem. Soc.* **1991**, *112*, 7826−7828.
(180) Liu, K. E.; Johnson, C. C.; Newcomb, M.; Lippard, S. J. *J. Am. Chem. Soc.* **1993**, *115*, 939−947.
(181) Tian, G.; Berry, J. A.; Klinman, J. P. *Biochemistry* **1994**, *33*, 226−234.
(182) Balch, A. L. *Inorg. Chim. Acta* **1992**, *297*, 297−307.
(183) Traylor, T. G.; Traylor, P. S. In *Active Oxygen in Biochemistry*; Valentine, J. S., Foote, C. S., Greenberg, A., Liebman, J. F., Eds.; Blackie Academic and Professional, Chapman and Hall: Glasgow, U.K., 1995; pp 84−187.
(184) Watanabe, Y.; Groves, J. T. In *The Enzymes*; Sigman, D. S., Boyer, P. D., Eds.; Academic Press: Orlando, 1992; pp 405−452.
(185) Lubben, M.; Meetsma, A.; Wilkinson, E. C.; Feringa, B.; Que, L., Jr. *Angew. Chem. Int. Ed. Engl.* **1995**, *34*, 1512−1514.
(186) Ménage, S.; Wilkinson, E. C.; Que, L., Jr.; Fontecave, M. *Angew. Chem. Int. Ed. Engl.* **1995**, *34*, 203−205.
(187) Kim, J.; Larka, E.; Wilkinson, E. C.; Que, L., Jr. *Angew. Chem. Int. Ed. Engl.* **1995**, *34*, 2048−2051.

CR960039F